First name and name: Jianqiang Zhou
Email address: Jqzhou_hit@hotmail.com

Title of the research project:
Progress of the theoretical description of photoemission in small systems: a model study

Host institution:
Ecole Polytechnique
Laboratoire des Solides Irradiés
91128 Palaiseau cedex
France

Laboratory and research group:
Laboratoire des Solides Irradiés
Theoretical Spectroscopy Group
http://etsf.polytechnique.fr/

Advisers:
Professor or lab director: Lucia Reining (lucia.reining@polytechnique.fr)
Other advisers: Claudia Rödl (claudia.roedl@polytechnique.edu)

Defense date: Monday, July 9, 2012

Progress in the theoretical description of photoemission in small systems: a model study
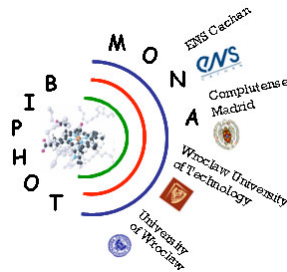
Jianqiang Zhou

MONABIPHOT Erasmus Mundus

ENS de Cachan

A thesis submitted for the degree of

Master of MONABIPHOT

Monday, July 9, 2012

I would like to dedicate this thesis to my wife and my parents.

Acknowledgements

Abstract

The electronic structure of solids can be probed by different types of spectro-scopies. Here we focus our discussion on photoemission spectroscopy and how it can be understood theoretically. Direct or inverse photoemission, which removes or adds one electron to the system, respectively, can be described by the one-particle Green's function. Thereby, we avoid the full solution of the many-electron problem. Approximate methods for the calculation of the Green's function have been studied for many years, and many different the-oretical approaches have been proposed. The GW approximation, developed by L. Hedin in 1965, is a well established approach for describing the quasi-particle peaks in the spectral function. The cumulant expansion, derived from model systems, is a promising approach for describing the photoemis-sion satellites. However, approximations for describing the satellite structure are still under investigation.

Other researchers in our group have already combined the cumulant expan-sion with the GW quasiparticle correction when modeling bulk silicon. They obtained very good agreement with experimental results for both the quasi-particle peaks and the satellite structure. However, the derivation of this approach uses some rough approximations whose validity has to be investi-gated.

As a test bed, we study the Hubbard model, which is widely used to deal with the physics of strongly correlated materials. Specifically, we choose the Hubbard molecule (the one-electron, two-site Hubbard model) to investigate the performance of this approach in a finite system. This model is very useful for evaluating the validity of different flavors of the cumulant expansion and the GW approximation, since the exact Green's function, and therefore also the spectral function, for this model molecule is known.

Contents

Chapter 1

Introduction

In this chapter, we start from the motivation of this work. Next we introduce direct (inverse) photoemission spectroscopy ((I)PES) focusing on the physical processes and terminology. The following section addresses the definition of the one-particle Green's function, explained in relation to (I)PES processes. In the fourth section, the cumulant expansion approximation is introduced. We also present one past work related to bulk silicon, a result which motivated our work on the cumulant expansion. In the last section, we introduce the two-site Hubbard model from its origin and its Hamiltonian in second quantization. We will use this model to evaluate the performance of the cumulant expansion approximation as well as combined with the GW quasiparticle correction.

1.1 Motivation

Spectroscopy owes its origin to the discovery of the photoelectric effect by Hertz and its explanation by Einstein, which earned him the Nobel prize. The interaction between matter and radiation (including electrons, light, x-rays, lasers, and other modern photon sources) is the key to study a vast number of materials, ranging from solids to atomic and nanoscale systems. In spectroscopy experiments, we perturb the sample with a beam of particles (photons or electrons) and measure the energy (or other properties) of the outgoing particles (again photons or electrons) (Table 1.1). From these processes we can determine the elementary excitations that the perturbation induces in the system. Therefore, spectroscopy can help us to obtain a lot of information about the properties of the materials, which allows us to predict the possible applications for these materials in industry. In this work, we focus our discussion on direct or inverse photoemission, which can be described directly by the one-particle Green's function.[1]

A typical photoemission experiment is performed at a synchrotron. Fig. (1.1) shows the scheme of the synchrotron SOLEIL. I have been there once for visiting before I started my work. From this visit, I got a lot of information about PES experiments. I also learned that the cost of doing these experiments is several millions of euros per

---

[1]The definition of the one-particle Green's function will be introduced later and can be found in any textbook on many-body physics such as "Many-particle theory" written by E. K. U. Gross.

Table 1.1: Classification of different kinds of spectroscopies.

Spectroscopy class	IN	OUT	Number of electrons in the sample
Direct photoemission	photon	electron	$N \to N-1$
Inverse photoemission	electron	photon	$N \to N+1$
Reflection	photon	photon	$N \to N$
Electron energy loss	electron	electron	$N \to N$

window[1] per year. How great would it be if we could get all the information that results from PES experiments just by a theoretical spectroscopy calculation?

http://www.synchrotron-soleil.fr/
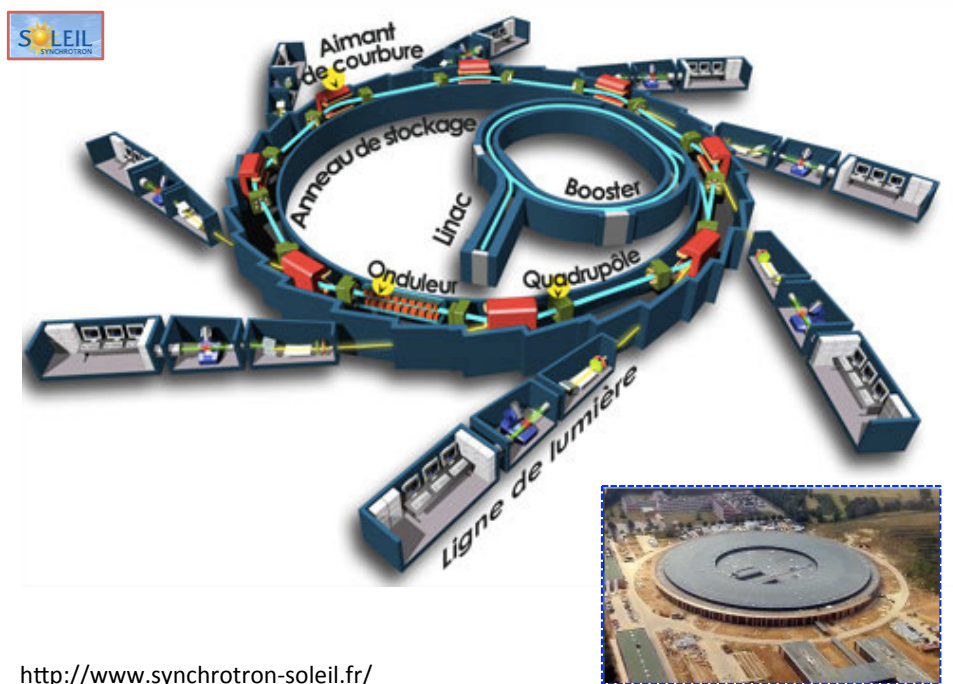
Figure 1.1: Schematic of the synchrotron SOLEIL in France

Nowadays theoretical spectroscopy[2] has become one of the most active research fields in condensed matter physics. It also has a lot of achievements on material science. For example, theoretical spectroscopy has explained the stability of optical absorption in CIGS solar-cells [1], or suggested ways to optimize phase change materials in optical data storage [2]. Also, the band gap of InN was predicted by theoretical spectroscopy

---

[1]Ligne de lumière in Fig. (1.1) where we get the x-ray from synchrotron and do our experiment.
[2]See http://www.etsf.eu/

before it could be measured experimentally because the sample quality was too poor [3].

In addition, theoretical spectroscopy can help us interpret experimental data and analyze the information from experimental results. For example, Fig. (1.2) depicts the data produced by a synchrotron experiment. It shows the measured electron counts in function of photon energy and photoelectron kinetic energy. In this figure, there is a lot of information to be analyzed.
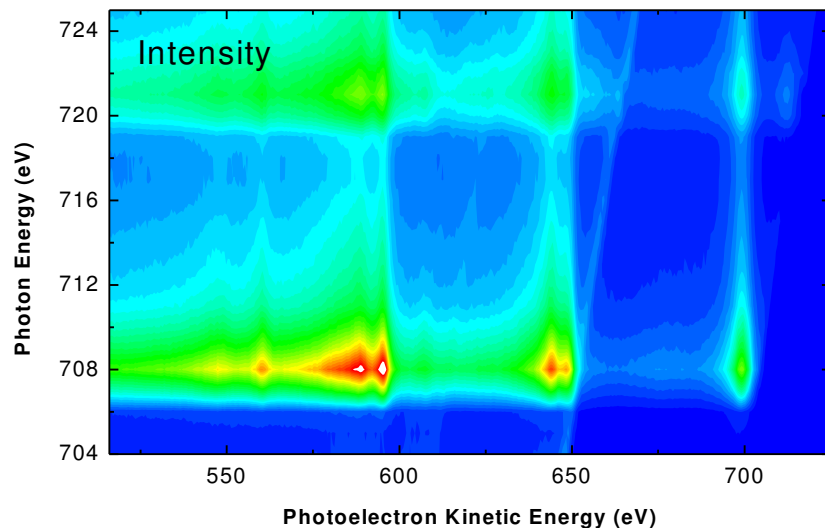
Figure 1.2: Experimental spectrum of bulk iron taken at the LURE synchrotron by F. Sirotti (unpublished).

Last but not least, because the experimental results for some materials are still missing, reliable theoretical simulations can help us predict the properties of new materials, which can optimize the process (time and money) for finding proper materials for the corresponding application. In addition, it is possible to achieve remarkable technological and fundamental breakthroughs via theoretical spectroscopy, such as new functionality (optoelectronics) or biological applications.

1.2   Direct and inverse photoemission spectroscopy

In a PES experiment, we irradiate the sample with photons (e.g. x-rays) of energy $h\nu$ to excite and emit electrons. By measuring the kinetic energy of the outgoing electrons, one has access to the electronic properties of the system.

If the electrons in the sample were independent particles, each emitted electron would contribute just to a delta peak in the spectrum, in correspondence to the one-particle energy level it was occupying in the system. However, the world is not so easy to understand because of the many-body effects. In real materials, electrons can never be

treated as independent particles, due to the Coulomb interaction. The emitted electron leaves a hole (i.e., a positive charge in correspondence to a depletion of negative charge) in the system. The presence of the hole induces a relaxation of the other electrons that screen this new positive charge (Fig. (1.3)). Therefore, the measured kinetic energy of the emitted electron is different from the independent particle situation. This in turn will lead to a shift and a renormalization of the independent particle peak, which broadens and loses part of its weight. When in the spectrum a main structure is still identifiable as
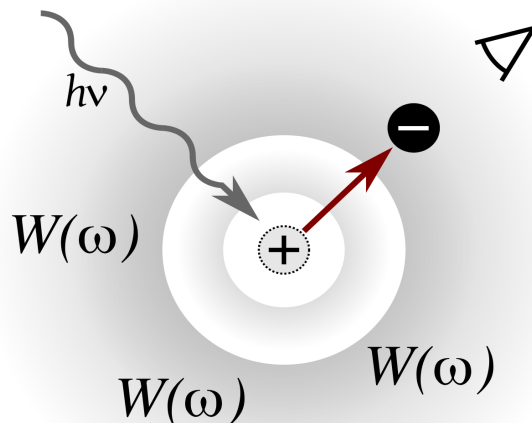
Figure 1.3: The diagram represents the excitation of plasmon satellites in PES in the electronic system. After the incoming photon ($h\nu$) induces one emitted electron, one positively charged hole will be left in the sample which induces relaxations of other electrons in the sample as well as other collective charge excitations (plasmons). The one-particle Green's function (see section 1.3) describes the propagation of particles, and the dynamically screened Coulomb interaction W represents the effective interaction between particles.

deriving from the independent particle peak, it can be still associated to a one-particle-like excitation, and we call this a *quasiparticle* peak. One can describe quasiparticle excitations by means of a one-particle Schrödinger equation with a complex, non-local, and frequency dependent effective potential.

The photon energy, besides creating and screening the hole, can be used also to simultaneously induce other excitations (mostly *plasmon excitations*) in the system. The excitations are observable in the spectrum, appearing as *satellites* at lower energies. In fact, the electron is emitted with a smaller kinetic energy compared with the independent particle situation.

In IPES, an electron is absorbed instead of a photon, and the emitted particle is a

photon. However the physics inside remains the same as PES. The electron is surrounded by a positively charged polarization cloud. The positive screening charge and the bare electron form a quasiparticle which weakly interacts with other quasiparticles via a screened, rather than the bare, Coulomb potential. In IPES the quasiparticle excitation will give part of its energy to the satellites at higher energies in the spectrum.

1.3 Green's function in many-body physics and the spectral function

The (I)PES process can be described by the one-particle Green's function. The definition of the zero-temperature, equilibrium, time-ordered, one-particle Green's function for a fermion reads [4]

$$G(12) = -i\langle \Psi_0^N | T[\psi_H(1)\psi_H^\dagger(2)] | \Psi_0^N \rangle \tag{1.1}$$

Here and throughout the thesis, we always use atomic units ($\hbar = e^2 = m_e = 1$). In Eq. (1.1) the index (1), for the sake of compactness, includes the space, spin, and time variables: $(1) = (x_1 t_1) = (r_1 \sigma_1 t_1)$. The N-particle ground-state wavefunction of the system is denoted by $|\Psi_0^N\rangle$. The field operator in the *Heisenberg picture*[1] that annihilates (adds) one particle at space, time and spin (xt) is given by $\psi_H(xt)$ $(\psi_H^\dagger(xt))$. T is the time-ordering operator.

If we write out the time-ordering operator using the step function we can express the Green's function as follows:

$$
\begin{aligned}
G(12) &= -i\theta(t_1 - t_2)\langle \Psi_0^N | \psi_H(1)\psi_H^\dagger(2) | \Psi_0^N \rangle + i\theta(t_2 - t_1)\langle \Psi_0^N | \psi_H^\dagger(2)\psi_H(1) | \Psi_0^N \rangle \\
&= G^{>(e)}(12)\theta(t_1 - t_2) + G^{<(h)}(12)\theta(t_2 - t_1)
\end{aligned}
\tag{1.2}
$$

in which $\theta(t)$ is the step function

$$
\theta(t) = \begin{cases} 1 & \text{if } t > 0 \\ 0 & \text{if } t < 0 \end{cases}
$$

and $G^{>(e)}(12)$ and $G^{<(h)}(12)$ are the so-called *greater* (*electron*) and *lesser* (*hole*) Green's functions.

The one-particle Green's function expresses the probability amplitude for an electron (a hole) which at time $t_2(t_1)$ is added to the system (in its ground state) in $r_2(r_1)$ with spin $\sigma_2(\sigma_1)$ to be found at $r_1(r_2)$ with spin $\sigma_1(\sigma_2)$ at a time $t_1 > t_2$ $(t_2 > t_1)$. For this reason, in literature the *greater* Green's function is sometimes called the *electron* Green's function G^e, and the *lesser* Green's function is called the *hole* Green's function G^h. The electron Green's function describes the IPES process and the hole Green's function describes the PES process (see Fig. (1.4)).

---

[1]There are three pictures, namely the Heisenberg, Schrödinger and interaction picture, which can be transformed into each other.
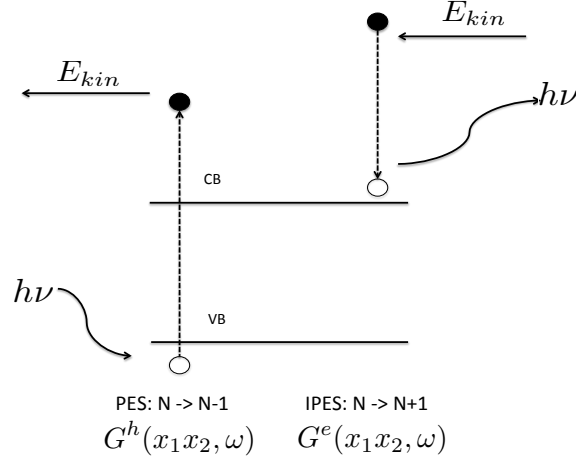
Figure 1.4: Schematic representation of PES (IPES) and the connection with the Green's function (see Eq. (1.2)). Here, E_{kin} is the kinetic energy of the electron and $h\nu$ is the photon energy. In an IPES process, we add one electron to our system. It means the electron propagates from one state to the other state as described by the electron Green's function. In PES, we remove one electron from our system, which corresponds to adding one hole to our system, and can be described by the hole Green's function.

In this thesis, we mainly work with the Lehmann representation of the one-particle time-ordered Green's function in frequency space:[1]

$$
\begin{aligned}
G(x_1 x_2, \omega) &= \sum_n \frac{\langle \Psi_0^N | \psi_S(x_1) | \Psi_n^{N+1} \rangle \langle \Psi_n^{N+1} | \psi_S^\dagger(x_2) | \Psi_0^N \rangle}{\omega - (E_n^{N+1} - E_0^N) + i\eta} \\
&+ \sum_n \frac{\langle \Psi_0^N | \psi_S^\dagger(x_2) | \Psi_n^{N-1} \rangle \langle \Psi_n^{N-1} | \psi_S(x_1) | \Psi_0^N \rangle}{\omega - (E_0^N - E_n^{N-1}) - i\eta}
\end{aligned}
\tag{1.3}
$$

----

[1]We use the Fourier transform in this work as

$$
\begin{aligned}
f(\omega) &= \int_{-\infty}^{+\infty} dt f(t) e^{iwt} \\
f(t) &= \frac{1}{2\pi} \int_{-\infty}^{+\infty} d\omega f(\omega) e^{-i\omega t},
\end{aligned}
$$

and the differential representations of the step function are

$$
\begin{aligned}
\theta(\tau) &= \lim_{\eta \to 0^+} -\frac{1}{2\pi i} \int_{-\infty}^{+\infty} d\omega \frac{e^{-i\omega\tau}}{\omega + i\eta} \\
\theta(-\tau) &= \lim_{\eta \to 0^+} \frac{1}{2\pi i} \int_{-\infty}^{+\infty} d\omega \frac{e^{-i\omega\tau}}{\omega - i\eta},
\end{aligned}
$$

where the infinitesimally small η is needed for the convergence of the integral.

where n labels the many-body states and ψ_S and $\psi_S^\dagger$ are the field operators in the Schrödinger picture, $|\Psi_0^N\rangle$ and $E_0^{N=1}$ are the ground-state wavefunction and energy, respectively, $|\Psi_n^{N+1}\rangle$ and E_n^{N+1} are the wavefunctions and energies after adding one electron in our system, and $|\Psi_n^{N-1}\rangle$ and E_n^{N-1} are the wavefunctions and energies after removing one electron from our system. Here $\eta \to 0^+$ comes from the differential form of the step function, whose sign distinguishes between the hole propagation $(-i\eta)$ and electron propagation $(+i\eta)$.

This representation of the Green's function is in real space. For our purpose, we need to transform it into a discrete basis set (e.g. the site basis in section 1.5). We can write the Green's function in the site basis using:

$$G_{ij} = \langle i|G(x_1 x_2)|j\rangle = \int dx_1 dx_2 \phi_i^*(x_1) G(x_1 x_2) \phi_j(x_2). \tag{1.4}$$

The field operator can be written as:

$$\psi_S(x) = \sum_i c_i \phi_i(x) \tag{1.5}$$

$$\psi_S^\dagger(x) = \sum_i c_i^\dagger \phi_i^*(x). \tag{1.6}$$

Therefore, we have

$$G_{ij}(\omega) = \sum_n \frac{\langle \Psi_0^N|c_i|\Psi_n^{N+1}\rangle \langle \Psi_n^{N+1}|c_j^\dagger|\Psi_0^N\rangle}{\omega - (E_n^{N+1} - E_0^N) + i\eta} + \sum_n \frac{\langle \Psi_0^N|c_j^\dagger|\Psi_n^{N-1}\rangle \langle \Psi_n^{N-1}|c_i|\Psi_0^N\rangle}{\omega - (E_0^N - E_n^{N-1}) - i\eta}, \tag{1.7}$$

where c_i and $c_j^\dagger$ are the so called *creation* and *annihilation* operators in the new basis set. The spin index is included in the index i and j here.

Finally, the imaginary part of the Green's function determines the spectral function A in frequency domain:

$$A(x_1 x_2, \omega) = \frac{1}{\pi} |\Im G(x_1 x_2, \omega)| \tag{1.8}$$

Since

$$\lim_{\eta \to 0^+} \frac{1}{\omega - \epsilon \pm i\eta} = \mathcal{P}\frac{1}{\omega - \epsilon} \mp i\pi\delta(\omega - \epsilon), \tag{1.9}$$

where $\mathcal{P}$ is the Cauchy principle value, the spectral function has δ peaks at the excitation energies ϵ. The intensity of those peaks is determined by the matrix elements in the numerator of the Green's function. We can see that, the spectral function reflects the excitation energies of the system that occur in direct and inverse photoemission.

1.4 Cumulant expansion approximation

The name cumulant expansion approximation was introduced by Langreth in 1970 [5], building up on earlier works of Hedin *et al.*[6]. In [5], an exact expression for the core

(hole) one-particle Green's function of a model Hamiltonian is derived, which has an exponential form (See Eq. (3.33) in chapter 3) and yields a spectrum containing a quasiparticle δ peak and a series of satellites, representing the different plasmon excitations. Each of the satellites has a different intensity, which depends on the probability for the corresponding plasmon excitation to happen.

In early works [7], researchers used the cumulant expansion approximation to reproduce satellites, while the GW approximation performs well for quasiparticle peaks [8]. The researchers in [9] developed a theory that combines the cumulant expansion with GW for solids. It yields excellent results for bulk silicon as shown in Fig. (1.5).
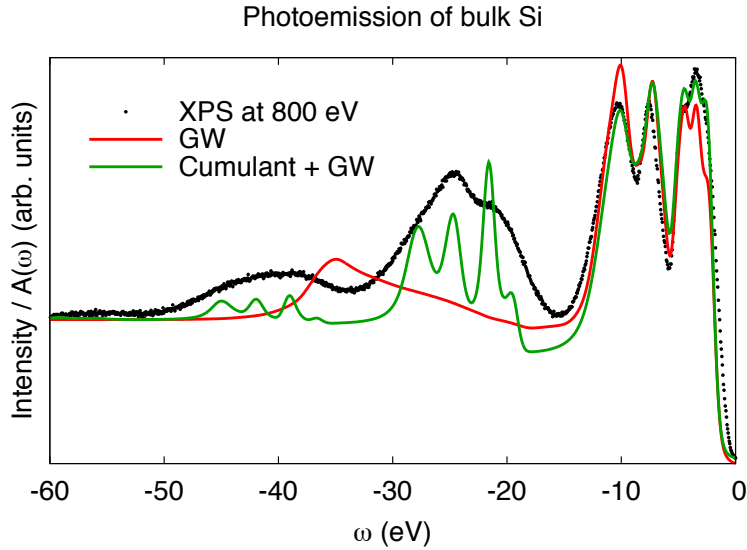
Figure 1.5: The performance of the combined approach (GW for the quasiparticles and cumulant expansion for the satellites) in comparison to a pure GW approach and experimental data for bulk Si.

Inspired by this result, the idea of my work is to investigate the performance of this approach in a finite system, and to understand the effects of the approximations involved. The main scheme of this work is shown in Fig. (1.6).

1.5 Two-site Hubbard model

The Hubbard model [10; 11] is named after John Hubbard who introduced a Hamiltonian in order to model electronic correlations in narrow energy bands and proposed a number of approximations to treat the associated many-body problem. In this work, we study the Hubbard molecule, namely the two-site Hubbard model, with only two sites and one orbital per site at quarter filling, i.e., with one electron. To obtain the Hamiltonian for
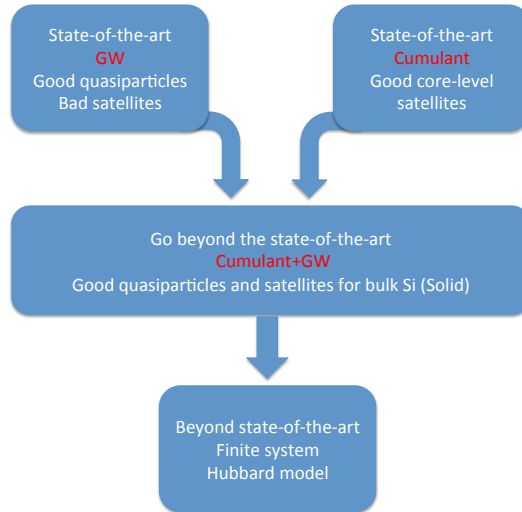
Figure 1.6: The main idea of this work: the state-of-the-art GW approximation is very successful in describing the quasiparticle peaks in the PES spectrum and the cumulant expansion is a very promising approach for describing the satellite structure. It has been shown that combining GW and the cumulant expansion has a very good agreement with the PES experiment for bulk Si who has infinite number of electrons. In this work we investigate this approach in a finite model system (two-site Hubbard model) and try to understand all the physics behind this approach.

our two-site Hubbard model, we need to start from the general form of the Hamiltonian in many-body physics (Eq. (1.10)).

A solid consists of ions and electrons condensed in a three-dimensional crystalline structure. Since the ions are much heavier than the electrons, it is often a good phenomenological starting point for the exploration of the electronic properties of solids to think the ions as forming a static lattice. In this approximation, the dynamics of the electrons is governed by the Hamiltonian as following in the *first quantization*:

$$H = \sum_{i=1}^{N} \left(\frac{p_i^2}{2m} + V(r_i) \right) + \sum_{1 \leq i < j \leq N} v(r_i, r_j), \tag{1.10}$$

where m is the mass of the electron and N the number of electrons in the system. $V(r_i)$ is the potential of the ions and we name it as external potential in this work. $v(r_i, r_j) = \frac{1}{|r_i - r_j|}$ is the Coulomb repulsion between electrons.[1] In our two-site Hubbard model, we only need to consider the case $N = 0, 1$, and 2 to describe electron removal

---

[1]The Coulomb interaction is spin-independent. Consequently this holds also for the Hartree potential and the screened Coulomb interaction.

and addition with respect to the one-electron system.

The general formula relating the first and second quantization is

$$H = \sum_\sigma \int dr \psi_\sigma^\dagger(r) h(r) \psi_\sigma(r) + \frac{1}{2} \sum_{\sigma\sigma'} \int \int dr dr' \psi_\sigma^\dagger(r) \psi_{\sigma'}^\dagger(r') v(r,r') \psi_{\sigma'}(r') \psi_\sigma(r), \quad (1.11)$$

where $h = p^2 + V$ is the one particle part of the Hamiltonian (1.10). The coefficient $1/2$ in the second term comes from the fact that i and j can be exchanged in second quantization form and both situations are equivalent, corresponding to $i < j$ in Eq. (1.10).

The central assumption of the Hubbard model is that all orbitals are strongly localized. That means the orbitals centered at different sites do not overlap, which allows us to write (using Eq. (1.4), (1.5), and (1.6))

$$v_{ijkl} = \int dr dr' \varphi_{i\sigma}^*(r) \varphi_{l\sigma}(r) v(r,r') \varphi_{j\sigma'}^*(r') \varphi_{k\sigma'}(r') = v_{ijji} \delta_{il} \delta_{jk} \quad (1.12)$$

for the matrix elements of the Coulomb interaction in the site basis. The second approximation involved in this model is that the Coulomb interaction is dominated by the on-site interaction, which allows us to write

$$v_{ijkl} = u \delta_{ij} \delta_{il} \delta_{ik}. \quad (1.13)$$

Here the on-site Coulomb interaction for the two-site Hubbard model is u. With these two approximations, we can write the Hamiltonian (1.10) for the two-site Hubbard model in site basis:

$$H = -t \sum_{\substack{i \neq j \\ i,j=1,2}} \sum_\sigma c_{i\sigma}^\dagger c_{j\sigma} + \frac{u}{2} \sum_{i=1,2} \sum_{\sigma\sigma'} c_{i\sigma}^\dagger c_{i\sigma'}^\dagger c_{i\sigma'} c_{i\sigma} + \epsilon_0 \sum_{\sigma,i=1,2} n_{i\sigma}, \quad (1.14)$$

where t is the hopping kinetic energy of electrons which represents the possibility for one electron to go from one site to the other. It comes from the off-diagonal elements of the kinetic energy in Eq. (1.10). ϵ_i is the orbital energy which comes from the diagonal elements of the kinetic energy and the ionic potential. Because in this model both sites are equivalent, we have $\epsilon_1 = \epsilon_2 = \epsilon_0$. $n_{i\sigma} = c_{i\sigma}^\dagger c_{i\sigma}$ is the number operator. The eigenstates of the system will be linear combinations of Slater determinants, which are denoted by the kets $|1;2\rangle$. The occupation of the sites 1 and 2 can be 0, $\uparrow$, $\downarrow$ or $\uparrow\downarrow$. At the beginning there is only one electron in our system, so the eigenstates can be $|0;\uparrow\rangle, |0;\downarrow\rangle, |\uparrow;0\rangle$, and $|\downarrow;0\rangle$. In this model, the vacuum state $|\Psi^{N=0}\rangle = |00\rangle$ has zero energy $E^{N=0} = 0$.

Chapter 2

Exact Green's function for the two-site Hubbard model

In this chapter, we calculate the exact Green's function for the two-site Hubbard molecule in both the site basis and the bonding-antibonding basis. We explain what information we can obtain from the one-particle Green's function via the energy-level diagrams and the spectral function. Finally, we discuss the IPES spectrum of adding one spin-down electron to show what is the quasiparticle peak and what is the satellite.

2.1 Exact Green's function in site basis

(*This part of work has been done by [12] and [13] separately, but I have redone all the calculations independently to try to have a good understanding of all the involved theories.*)

We already introduced the Lehmann representation of the Green's function in Eq. (1.7). Now we write this representation for the two-site Hubbard model in the site basis:

$$
\begin{aligned}
G_{ij\sigma}^{N=1}(\omega) \;=\; & \sum_n \frac{\langle \Psi_0^{N=1}|c_{i\sigma}|\Psi_n^{N=2}\rangle \langle \Psi_n^{N=2}|c_{j\sigma}^\dagger|\Psi_0^{N=1}\rangle}{\omega - (E_n^{N=2} - E_0^{N=1}) + i\eta} \\
+\; & \sum_n \frac{\langle \Psi_0^{N=1}|c_{j\sigma}^\dagger|\Psi^{N=0}\rangle \langle \Psi^{N=0}|c_{i\sigma}|\Psi_0^{N=1}\rangle}{\omega - (E_0^{N=1} - E^{N=0}) - i\eta},
\end{aligned}
\tag{2.1}
$$

where $|\Psi_0^{N=1}\rangle$ and $E_0^{N=1}$ are the ground-state wavefunction and energy, respectively. $|\Psi_n^{N=2}\rangle$ and $E_n^{N=2}$ are the wavefunctions and energies when there are two electrons in our system. $|\Psi^{N=0}\rangle$ and $E^{N=0}$ are the wavefunction and energy when there is no electron in our system.

From Eq. (2.1) we know that if we want to construct the one-particle Green's function for the one-electron system ($G_{ij\sigma}^{N=1}$) we need to know all the wavefunctions and energies for the one-electron (ground state), two-electron (adding one electron), and zero-electron (remove one electron) systems. Here we set the vacuum state $|\Psi^{N=0}\rangle = |0;0\rangle$ to zero

energy $E^{N=0} = 0$. In the following section, we derive the energies and wavefunctions for the one-electron and two-electron systems.

2.1.1 Wavefunctions and energies for one- and two-electron systems

We have already introduced the two-site Hubbard model Hamiltonian in Eq. (1.14). When there is only one electron in our system, this electron has four possibilities to be on one site or the other site, to be spin up or spin down. Therefore the possible one-electron states in the site basis are:

$$| \uparrow; 0\rangle, | \downarrow; 0\rangle, |0; \uparrow\rangle, |0; \downarrow\rangle. \tag{2.2}$$

Then we write the Hamiltonian (1.14) in this basis,[1] which results in a 4×4 matrix as shown below:

$$H^{N=1} = \begin{pmatrix} \epsilon_0 & 0 & -t & 0 \\ 0 & \epsilon_0 & 0 & -t \\ -t & 0 & \epsilon_0 & 0 \\ 0 & -t & 0 & \epsilon_0 \end{pmatrix}. \tag{2.3}$$

We can calculate all the eigenvectors (wavefunctions) and eigenvalues (energies) of this matrix and the results are shown in the following table:

Table 2.1: Eigenvalues and eigenvectors of one-electron system

$E_n^{N=1}/|\Psi_n^{N=1}\rangle$	$\mid \uparrow; 0\rangle$	$\mid \downarrow; 0\rangle$	$\mid 0; \uparrow\rangle$	$\mid 0; \downarrow\rangle$
$\epsilon_0 - t$	0	$1/\sqrt{2}$	0	$1/\sqrt{2}$
$\epsilon_0 - t$	$1/\sqrt{2}$	0	$1/\sqrt{2}$	0
$\epsilon_0 + t$	0	$1/\sqrt{2}$	0	$-1/\sqrt{2}$
$\epsilon_0 + t$	$1/\sqrt{2}$	0	$-1/\sqrt{2}$	0

Here, we choose our ground state such that there is one spin-up electron in our system. Therefore the ground-state wavefunction and energy are $|\Psi_0^{N=1}\rangle = 1/\sqrt{2}(| \uparrow; 0\rangle + |0; \uparrow\rangle)$ and $E_0^{N=1} = \epsilon_0 - t$, respectively. Actually we could have also chosen to have one spin-down electron in the ground state. Both situations are equivalent.

When we have two electrons in our system, there are six possibilities to build up two-particle states:

$$| \uparrow; \downarrow\rangle, | \downarrow; \uparrow\rangle, | \uparrow; \uparrow\rangle, | \downarrow; \downarrow\rangle, | \uparrow\downarrow; 0\rangle, |0; \uparrow\downarrow\rangle$$

If we write the Hamiltonian (1.14) in the two-particle basis, we obtain a 6×6 matrix:

$$H^{N=2} = \begin{pmatrix} 2\epsilon_0 & 0 & 0 & 0 & -t & -t \\ 0 & 2\epsilon_0 & 0 & 0 & t & t \\ 0 & 0 & 2\epsilon_0 & 0 & 0 & 0 \\ 0 & 0 & 0 & 2\epsilon_0 & 0 & 0 \\ -t & t & 0 & 0 & 2\epsilon_0 + u & 0 \\ -t & t & 0 & 0 & 0 & 2\epsilon_0 + u \end{pmatrix}. \tag{2.4}$$

---

[1]Here, we follow the convention $c^\dagger_{|\uparrow;0\rangle} c^\dagger_{|\downarrow;0\rangle} c^\dagger_{|0;\uparrow\rangle} c^\dagger_{|0;\downarrow\rangle} |0; 0\rangle = | \uparrow\downarrow; \uparrow\downarrow\rangle$.

The eigenvalues and eigenvectors of this matrix are shown in Table 2.2, where we have introduced the abbreviations $c = \sqrt{16t^2 + u^2}$, $a = \sqrt{2((16t^2/(c-u)^2)+1)}$, and $b = \sqrt{2((16t^2/(c+u)^2)+1)}$.

Table 2.2: Eigenvalues and eigenvectors of two-electron system

$E_n^{N=2}/\lvert\Psi_n^{N=2}\rangle$	$\lvert\uparrow;\downarrow\rangle$	$\lvert\downarrow;\uparrow\rangle$	$\lvert\uparrow;\uparrow\rangle$	$\lvert\downarrow;\downarrow\rangle$	$\lvert\uparrow\downarrow;0\rangle$	$\lvert0;\uparrow\downarrow\rangle$
$2\epsilon_0 + \frac{u-c}{2}$	$\frac{4t}{a(c-u)}$	$\frac{-4t}{a(c-u)}$	0	0	$1/a$	$1/a$
$2\epsilon_0 + \frac{u+c}{2}$	$\frac{-4t}{b(c+u)}$	$\frac{4t}{b(c+u)}$	0	0	$1/b$	$1/b$
$2\epsilon_0 + u$	0	0	0	0	$-1/\sqrt{2}$	$1/\sqrt{2}$
$2\epsilon_0$	0	0	0	1	0	0
$2\epsilon_0$	0	0	1	0	0	0
$2\epsilon_0$	$1/\sqrt{2}$	$1/\sqrt{2}$	0	0	0	0

2.1.2 Construct the Green's function in site basis

Now, we have everything we need to construct the one-particle Green's function. Inserting all the wavefunctions and energies and calculating the matrix elements (e.g. $\langle\Psi_0^{N=1}|c_{i\sigma}|\Psi_n^{N=2}\rangle$) in Eq. (2.1), we get all the elements of the Green's function matrix:

$$
G(\omega) = \begin{pmatrix}
G_{11\uparrow} & G_{12\uparrow} & 0 & 0 \\
G_{21\uparrow} & G_{22\uparrow} & 0 & 0 \\
0 & 0 & G_{11\downarrow} & G_{12\downarrow} \\
0 & 0 & G_{21\downarrow} & G_{22\downarrow}
\end{pmatrix},
\tag{2.5}
$$

where

$$
G_{ij\uparrow}(\omega) = \frac{(-1)^{i-j}}{2}\left[\frac{1}{\omega-(\epsilon_0+t)+i\eta} + \frac{(-1)^{i-j}}{\omega-(\epsilon_0-t)-i\eta}\right],
\tag{2.6}
$$

$$
G_{ij\downarrow}(\omega) = \frac{1}{2}\left[\frac{\left(\frac{4t}{a(c-u)}+\frac{1}{a}\right)^2}{\omega-(\epsilon_0+(u-c)/2+t)+i\eta} + \frac{\left(\frac{4t}{b(c+u)}-\frac{1}{b}\right)^2}{\omega-(\epsilon_0+(u+c)/2+t)+i\eta}\right]
$$

$$
+ \frac{(-1)^{i-j}}{4}\left[\frac{1}{\omega-(\epsilon_0+u+t)+i\eta} + \frac{1}{\omega-(\epsilon_0+t)+i\eta}\right].
\tag{2.7}
$$

Here we can see the one-particle Green's function is spin diagonal, which is a direct consequence of having a spin-independent external potential and a spin-independent Coulomb interaction. The spin-up block has both electron and hole parts and the spin-down block has only the electron part, which is consistent with the fact that there is only one spin-up electron in our system (That is why we can only create a spin-up hole.). From Eq. (2.6) and (2.7), we obtain the relation $G_{11} = G_{22}$ and $G_{12} = G_{21}$ for both spin-up and spin-down blocks because the sites in this Hubbard model are equivalent.

If we put $u = 0$ in Eq. (2.6) and (2.7), we can get the so-called non-interacting Green's function G_0:

$$G_{ij\uparrow}^0(\omega) \;=\; \frac{(-1)^{i-j}}{2}\left[\frac{1}{\omega - (\epsilon_0 + t) + i\eta} + \frac{(-1)^{i-j}}{\omega - (\epsilon_0 - t) - i\eta}\right], \qquad (2.8)$$

$$G_{ij\downarrow}^0(\omega) \;=\; \frac{(-1)^{i-j}}{2}\left[\frac{1}{\omega - (\epsilon_0 + t) + i\eta} + \frac{(-1)^{i-j}}{\omega - (\epsilon_0 - t) + i\eta}\right]. \qquad (2.9)$$

We can see $G_{ij\uparrow}^0 = G_{ij\uparrow}$ (Eq. (2.8) and (2.6)). This is because whenever we remove or add one spin-up electron, there can never be Coulomb interaction due to the purely on-site Coulomb interaction in this two-site Hubbard model.

2.2 Basis transformation from site basis to bonding-antibonding basis

Up to now, all our calculations have been carried out in the site basis which can be considered as an atomic-like basis set. Here, we introduce the bonding-antibonding basis which is conceptually similar to a molecular-orbital basis. The advantage of this new basis set is that the Green's function becomes diagonal (see Eq. (2.15)) which simplifies both the calculation and the interpretation of the results.

The bonding-antibonding basis functions are

$$\begin{aligned}
|\Psi_{b\uparrow}\rangle &= 1/\sqrt{2}(|\uparrow;0\rangle + |0;\uparrow\rangle) \\
|\Psi_{b\downarrow}\rangle &= 1/\sqrt{2}(|\downarrow;0\rangle + |0;\downarrow\rangle) \\
|\Psi_{a\downarrow}\rangle &= 1/\sqrt{2}(|\uparrow;0\rangle - |0;\uparrow\rangle) \\
|\Psi_{a\downarrow}\rangle &= 1/\sqrt{2}(|\downarrow;0\rangle - |0;\downarrow\rangle),
\end{aligned}$$

in which a and b represent the antibonding and bonding orbital, respectively.

Now we use the basis transformation to get the new Green's function matrix. The transformation equation is[1]

$$\langle\Psi_{l\sigma}|G(\omega)|\Psi_{m\sigma}\rangle = \sum_{\sigma'}\sum_{i,j}\langle\Psi_{l\sigma}|i\sigma'\rangle\langle i\sigma'|G(\omega)|j\sigma'\rangle\langle j\sigma'|\Psi_{m\sigma}\rangle, \qquad (2.10)$$

where l and m are the state indices representing the bonding (b) or the antibonding (a) orbital.

---

[1]With this transformation equation, we can transform all the one-particle quantities from site basis to bonding-antibonding basis.

The non-vanishing matrix elements of the Green's function in this basis are:

$$G_{bb\uparrow}(\omega) = \frac{1}{\omega - (\epsilon_0 - t) - i\eta} \tag{2.11}$$

$$G_{bb\downarrow}(\omega) = \frac{\left(\frac{4t}{a(c-u)} + \frac{1}{a}\right)^2}{\omega - (\epsilon_0 + (u-c)/2 + t) + i\eta} + \frac{\left(\frac{4t}{b(c+u)} - \frac{1}{b}\right)^2}{\omega - (\epsilon_0 + (u+c)/2 + t) + i\eta} \tag{2.12}$$

$$G_{aa\uparrow}(\omega) = \frac{1}{\omega - (\epsilon_0 + t) + i\eta} \tag{2.13}$$

$$G_{aa\downarrow}(\omega) = \frac{1}{2}\left(\frac{1}{\omega - (\epsilon_0 + u + t) + i\eta} + \frac{1}{\omega - (\epsilon_0 + t) + i\eta}\right). \tag{2.14}$$

We only write these four elements because all other elements are zero. The Green's function matrix in bonding-antibonding basis is a diagonal matrix reading as follows:

$$G(\omega) = \begin{pmatrix} G_{bb\uparrow} & 0 & 0 & 0 \\ 0 & G_{bb\downarrow} & 0 & 0 \\ 0 & 0 & G_{aa\uparrow} & 0 \\ 0 & 0 & 0 & G_{aa\downarrow} \end{pmatrix} \tag{2.15}$$

2.3 Energy-level diagrams

Before we introduce the spectral function and the interpretation of each Green's function element, we first construct the energy-level diagrams for the one- and two-electron systems.

To draw the energy-level diagrams for the Hubbard molecule with one and two electrons, we first consider the atomic limit, i.e., when the two sites are infinitely far away from each other. In this case, it is impossible for the electron to go from one site to the other. That means $t \to 0$. In this situation, there will be only one energy level left for the one-electron system, which is ϵ_0 as shown in Table 2.1. While for the two-electron system, there are two energy levels left in atomic limit which are $2\epsilon_0$ and $2\epsilon_0 + u$ as shown in Table 2.2. When the two sites come closer to each other (t is not zero any more) the energy levels will split into two for the one-electron system and four for the two-electron system as shown in Fig. (2.1).

We give a brief discussion about the Green's function with the energy-level diagrams.[1]

If we remove the ground-state electron (spin-up electron) from our system, our system will lose the energy $\epsilon_0 - t$. Because we know from the one-electron energy-level diagram (Fig. (2.1)) that, this spin-up electron is in the bonding orbital whose energy is $\epsilon_0 - t$. It means that at the beginning, our system has the energy $\epsilon_0 - t$. But if we remove this electron, the energy of our system will be zero. We can imagine this process as a photoemission process, where one peak would appear at $\epsilon_0 - t$ in the spectrum. If we calculate the spectral function (via Eq. (1.8)) for electron removal, the only contribution

---

[1]This discussion is my own interpretation of each Green's function matrix element in the two-site Hubbard model. It expands on previous explanations.
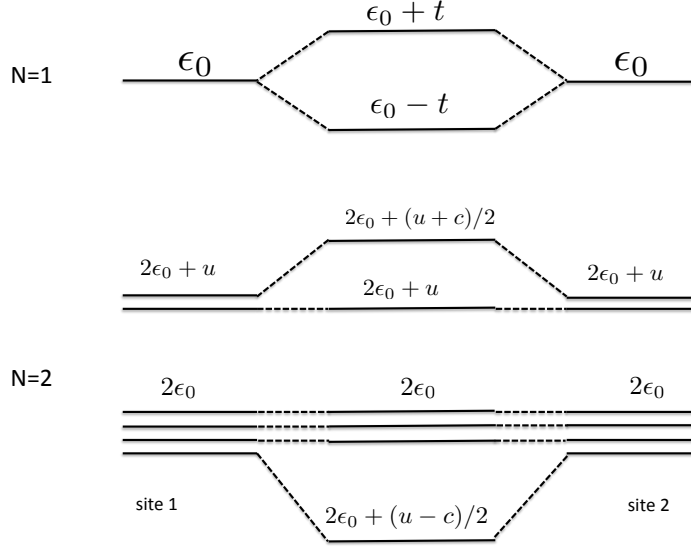
Figure 2.1: Energy-level diagrams for one-electron and two-electron systems. The bonding orbital has the energy $\epsilon_0 - t$ and the antibonding orbital has the energy $\epsilon_0 + t$.

arises from $G_{bb\uparrow}(\omega)$. So $G_{bb\uparrow}(\omega)$ describes the process when we remove this ground-state electron from our system.

Then we consider another situation: We add one electron to our system corresponding to an inverse photoemission process. From the energy-level diagram (Fig. (2.1)), we can guess there should be four peaks appearing at $2\epsilon_0 - (\epsilon_0 - t) = \epsilon_0 + t$ (peak 1 in Fig. (2.2)), $2\epsilon_0 + u - (\epsilon_0 - t) = \epsilon_0 + u + t$ (peak 2 in Fig. (2.2)), $2\epsilon_0 + (u-c)/2 - (\epsilon_0 - t) = \epsilon_0 + t + (u-c)/2$ (peak 3 in Fig. (2.2)), and $2\epsilon_0 + (u+c)/2 - (\epsilon_0 - t) = \epsilon_0 + t + (u+c)/2$ (peak 4 in Fig. (2.2)). The four electron addition peaks in the spectral function are due to the contributions from $G_{bb\downarrow}$, $G_{aa\uparrow}$, and $G_{aa\downarrow}$. Here, we can discuss the situations with different spins separately.

First, if we add one spin-up electron to our system, this electron can only go to the site which is empty at the beginning and finally stay in the antibonding orbital according to the Pauli exclusion principle. In this case the total energy of our system will be $(\epsilon_0 - t) + (\epsilon_0 + t) = 2\epsilon_0$ as show in Fig. (2.1). There will be one peak appearing at $2\epsilon_0 - (\epsilon_0 - t) = \epsilon_0 + t$ (peak 1 in Fig. (2.2)) in the spectrum, which is calculated from $G_{aa\uparrow}$.

In the case we add one spin-down electron in our system, this electron can stay in the bonding orbital or the antibonding orbital. When it stays in the antibonding orbital ($G_{aa\downarrow}$) there are two possibilities (two poles). The first possibility is that this electron stays on the same site as the ground-state electron, where the total energy of our system will be $(\epsilon_0 - t) + (\epsilon_0 + t + u) = 2\epsilon_0 + u$ and the peak will appear at $2\epsilon_0 + u - (\epsilon_0 - t) = \epsilon_0 + u + t$. Another possibility is that this spin-down electron is on the other site which is empty at

$$\omega_1 = \epsilon_0 + t$$
$$\omega_2 = \epsilon_0 + u + t$$
$$\omega_3 = \epsilon_0 + (u - c)/2 + t$$
$$\omega_4 = \epsilon_0 + (u + c)/2 + t$$
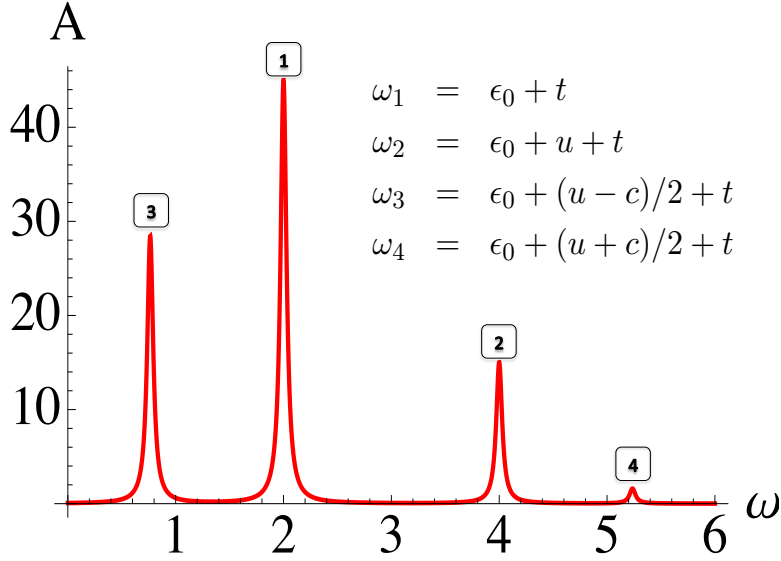
Figure 2.2: The spectral function for electron propagation. This corresponds to the IPES process where we add one electron to the system. We plot $A^e(\omega) = |\Im(G_{bb\downarrow} + G_{aa\uparrow} + G_{aa\downarrow})|$. Here we set $\epsilon_0 = t = 1$ and $u = 2$.

the beginning. In this situation, the total energy of our system will be $2\epsilon_0$ and the peak will appear at $\epsilon_0 + t$. We can get these two peaks in the spectral function calculated from $G_{aa\downarrow}$ (peak 1 and peak 2 in Fig. (2.2)). The possibility for this spin-down electron to be on each site is the same (the numerators are the same in Eq. (2.14)).

When this spin-down electron stays in the bonding orbitals, the situation becomes very interesting. Because we first need to find the effective Coulomb interaction between two electrons on the same orbital (on the same site or on the different sites), which is not the bare Coulomb interaction u anymore. When the sites and orbitals combine together we need to define a new effective Coulomb interaction to describe the interaction between electrons on the same orbital. Let's say u' is the on-site and on-orbital effective Coulomb interaction and we have $u' = 2t + (c - u)/2$.[1] u'' is the off-site and on-orbital effective Coulomb interaction and we have $u'' = 2t + (u - c)/2$.[2] With these two newly defined interactions, we can interpret $G_{bb\downarrow}$ as: When the incoming spin-down electron arrives at the same site as the ground-state spin-up electron and both of them stay in the bonding orbital, the total energy of our system will be $2\epsilon_0 + (u + c)/2$, which yields a peak at $\epsilon_0 + t + (u + c)/2$. While if the incoming electron arrives at the empty site and the bonding orbital, the total energy of our system is $2\epsilon_0 + (u - c)/2$ and there will be one peak appearing at $\epsilon_0 + t + (u - c)/2$ (peak 3 and peak 4 in Fig. (2.2)). Apparently, when both electrons are in the bonding orbital, they prefer to be off-site (From the intensity

---

[1] In this case, the total energy of our system should be $2(\epsilon_0 - t) + u + u' = 2\epsilon_0 + (u + c)/2$.

[2] Now, the total energy of our system is $2(\epsilon_0 - t) + u'' = 2\epsilon_0 + (u - c)/2$

17

of these two peaks we can say this.)

2.4 Spectral function calculated from the exact Green's function

In this section, we take the process of adding one spin-down electron to our system as an example to show the different properties of quasiparticle peaks and satellites.

For the spectral function the two important properties are the positions of the peaks and their intensities. The peak position results from the denominator of the Green's function and it tells us the excitation energy. The intensity comes from the numerator, which describes the probability for this excitation to occur. In this work, when $u/t = 2$ is corresponding to the system with normal interaction and $u/t = 4$ is the strong interaction system.
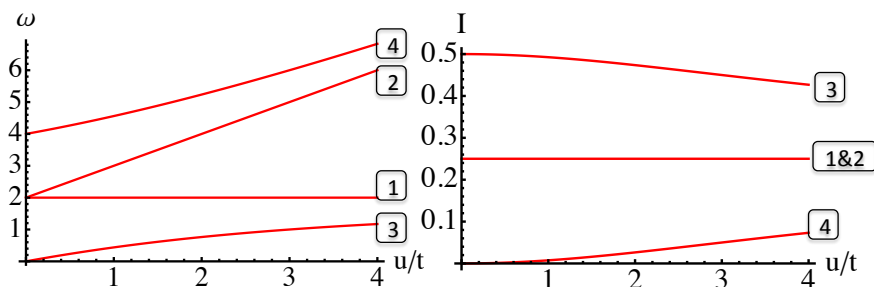
Figure 2.3: IPES peak positions (left) and intensities (right) for adding a spin-down electron in dependence on u/t.

From the left plot in Fig. (2.3), we know all the peaks except peak 1 will have a blue shift when the Coulomb interaction becomes stronger and stronger. This means we need more energy to excite the system with stronger correlation. From the right plot we know that in the absence of interaction $u = 0$, the intensity of peak 4 will be zero. Its intensity becomes bigger with increasing Coulomb interaction, which is consistent with the definition of a satellite peak in section (1.2). In the non-interacting limit, peak 1 and peak 2 are degenerate and only one peak is visible (left plot when $u = 0$). That is why we can only see two peaks (peak 1 and 2 are in the same position and peak 4 has zero intensity) in the spectral function (green plot in Fig. (2.4)) for $u = 0$. The peaks 1, 2, and 3 are the so-called *quasiparticle* peaks, because they have non-vanishing intensity in the absence of interaction. Satellites can only be excited in the presence of interaction because they are collective many-body excitations. That is why peak 4 is identified as a satellite.
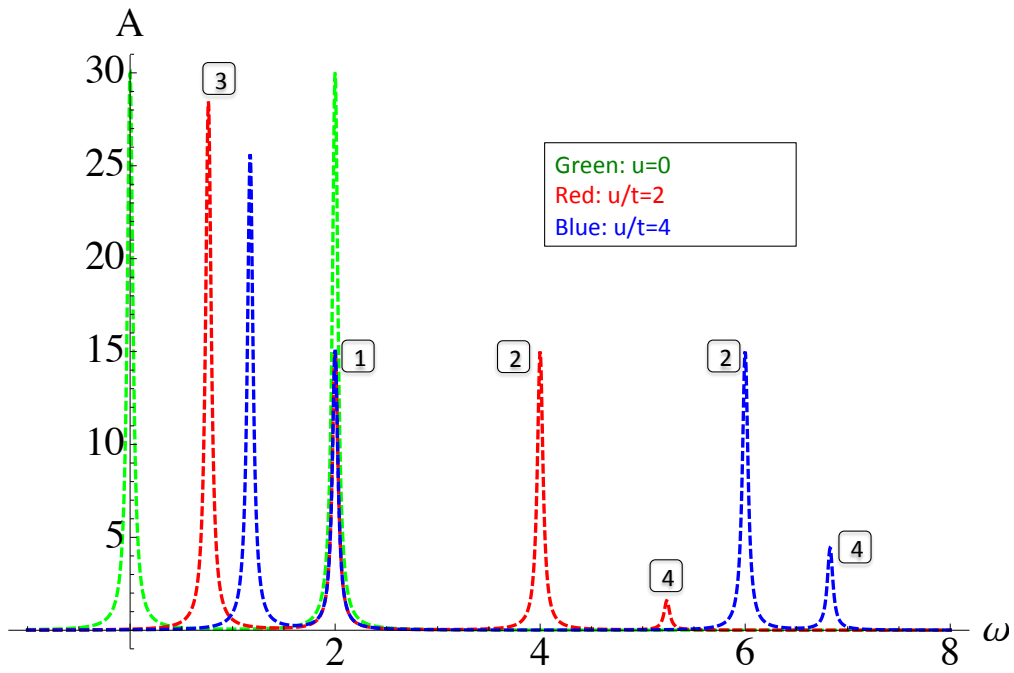
Figure 2.4: The spectral function for adding a spin-down electron in different interactions. Here we set $\epsilon_0 = t = 1$. When $u = 0$ (non-interacting case), there are only two peaks. When the Coulomb interaction u becomes bigger and bigger, all the peaks have a blue shift except peak 1. In our model $u/t = 2$ describes a material with normal interaction and $u/t = 4$ is a system with strong interaction.

Chapter 3

Cumulant expansion

In this chapter, we calculate the cumulant Green's function for the two-site Hubbard model. We start from the equation of motion (EOM) of the one-particle Green's function to introduce the so-called cumulant expansion approximation. In the second section, we derive the cumulant expansion for the two-site Hubbard model. To calculate the cumulant Green's function, we first need to calculate the Hartree Green's function and the screened Coulomb interaction in both the site basis and the bonding-antibonding basis. The scheme of this chapter is show in Fig. (3.1).

3.1   General cumulant expansion

When we calculated the exact Green's function for the Hubbard molecule, we already knew the exact ground state of our system. However, in a real system, it is impossible to find the exact ground state due to the infinite number of electrons. What can we do if we do not know the exact ground state, but we still want to calculate the Green's function?

The main idea is this: First, we determine the time evolution of the one-particle Green's function from the time evolution of the field operators. In this equation, a two-particle Green's function appears. Second, we use an external perturbation potential φ to perturb our system, which allows us to express the two-particle Green's function as a functional derivative of the one-particle Green's function. Then we can write the EOM of the one-particle Green's function, from which we will be able to get the information of our system. After we get the Green's function containing the external perturbation, we can set the external perturbation to zero to get the equilibrium Green's function. So
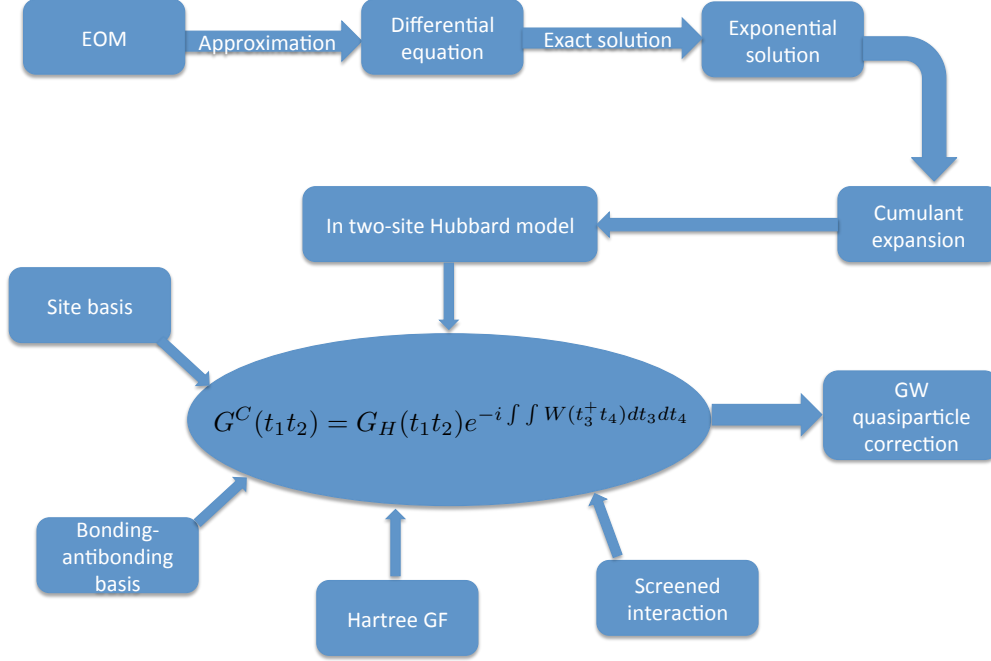
Figure 3.1: This scheme represents the idea of the cumulant expansion and the combination with GW quasiparticle corrections. We start from the very beginning of the equation of motion of the one-particle Green's function (EOM) (Eq. (3.1)). Then we add approximations until we find an equation which we can solve exactly (Eq. (3.3)). The solution of Eq. (3.3) has an exponential form which we Taylor-expand to get our cumulant result. We next calculate the Hartree Green's function and the screened Coulomb interaction (RPA and exact) in different basis sets, so we can get the cumulant Green's functions with several different ingredients. Finally, we add GW quasiparticle corrections for all conditions to see the performance of our approach (in chapter 4).

we start from the EOM (Eq. (3.1)) [14].

$$
\begin{aligned}
G(12; [\varphi]) = G_0(12) \quad & + \quad \int d3 G_0(13) V_H(3; [\varphi]) G(32; [\varphi]) \\
& + \quad \int d3 G_0(13) \varphi(3) G(32; [\varphi]) \\
& + \quad i \int d3 d4 G_0(13) v(3^+4) \frac{\delta G(32; [\varphi])}{\delta \varphi(4)},
\end{aligned} \tag{3.1}
$$

where φ is the external perturbation, G_0 is the non-interacting Green's function (Eq. (2.8) and (2.9)), $v(12) = v(r_1 r_2) \delta(t_1 - t_2)$ is the Coulomb potential between electrons,

and $V_H(3) = -i \int d4 v(3^+4) G(44^+; [\varphi])$ is the Hartree potential, which I will explain later in this chapter.[1] Notice that since the Hartree potential contains the Green's function, Eq. (3.1) is non-linear. Once this equation is solved, we can calculate the exact Green's function for any system (material). However, there is no exact way to solve this equation, at least until now.

Therefore, we need to find an approximate way to solve it. For the cumulant expansion, the approximations involved are what we called the *linearization approximation* and *diagonalization approximation*.

Using the linearization approximation,[2] Eq. (3.1) can be written as [15]:

$$
\begin{aligned}
G(12; [\bar{\varphi}]) = G_H^0(12) \quad &+ \quad \int d3 G_H^0(13) \bar{\varphi}(3) G(32; [\bar{\varphi}]) \\
&+ \quad i \int d3 d4 G_H^0(13) W(3^+4) \frac{\delta G(32; [\bar{\varphi}])}{\delta \bar{\varphi}(4)},
\end{aligned} \tag{3.2}
$$

where $W = \varepsilon^{-1} v$ is the screened Coulomb potential at vanishing φ with ε the dielectric function. G_H^0 is the Hartree Green's function containing the Hartree potential at vanishing φ, $\bar{\varphi} = \varepsilon^{-1} \varphi$ is the renormalized external perturbation.

Through this linearization, the screened interaction W becomes the central quantity of Eq. (3.2), which can be calculated in random-phase approximation (RPA).[3] For Eq. (3.2), we still do not know the exact solution, so we need to use a further approximation, i.e., the diagonalization approximation, which allows us to write Eq. (3.2) as [9]:

$$
\begin{aligned}
G(t_1 t_2; [\bar{\varphi}]) = G_H^0(t_1 t_2) \quad &+ \quad \int dt_3 G_H^0(t_1 t_3) \bar{\varphi}(t_3) G(t_3 t_2; [\bar{\varphi}]) \\
&+ \quad i \int dt_3 dt_4 G_H^0(t_1 t_3) W(t_3^+ t_4) \frac{\delta}{\delta \bar{\varphi}(t_4)} G(t_3 t_2; [\bar{\varphi}]). \tag{3.3}
\end{aligned}
$$

In the diagonalization, there is no longer a space index because we treat both G and G_H^0 as diagonal matrices in space on the same basis.[4] Now there is a problem because the results will depend on the basis set. Which basis is better and how can we choose the better basis? We will discuss this later in chapter 4.

---

[1]3^+ means that the time is $t_3 + \eta$. The small parameter $\eta \to 0^+$ is needed for this time ordering.

[2]$V_H = V_H^0 + \int \varphi v \chi$, where $\chi = \frac{\delta \rho}{\delta \varphi}$ is the response function and V_H^0 is the Hartree potential without the external potential. In the linearization, we write $V_H = V_H^0$ to linearize Eq. (3.1). But in this work to avoid more indices, we use V_H to represent V_H^0.

[3]In RPA, the screening is due to the non-interacting electron-hole pairs.

[4]It means the decoupling of the quantities for all space and spin or orbital coordinates, i.e.,

$$
\begin{aligned}
G(12) &= \sum_{kk'} G_{kk'}(t_1, t_2) \phi_k(r_1) \phi_{k'}^*(r_2) \approx \sum_k G_{kk}(t_1, t_2) \phi_k(r_1) \phi_k^*(r_2) \\
G_H^0(12) &= \sum_{kk'} G_{H;kk'}^0(t_1, t_2) \phi_k(r_1) \phi_{k'}^*(r_2) \approx \sum_k G_{H;kk}^0(t_1, t_2) \phi_k(r_1) \phi_k^*(r_2)
\end{aligned}
$$

The exact solution of Eq. (3.3) is:

$$
\begin{aligned}
G^C(t_1 t_2)|_{\varphi=0} &= G_H^h(t_1 t_2) e^{-i \int_{t_1}^{t_2} dt_3 \int_{t_3}^{t_2} dt_4 W(t_3^+ t_4)} \\
&+ G_H^e(t_1 t_2) e^{-i \int_{t_2}^{t_1} dt_3 \int_{t_2}^{t_3} dt_4 W(t_3^+ t_4)}
\end{aligned}
\tag{3.4}
$$

We call this Green's function, which includes linearization and diagonalization approximations, the cumulant Green's function G^C [9]. From here on, we write G_H instead of G_H^0 to avoid more indices.

3.2 Cumulant expansion for the two-site Hubbard model

To calculate the cumulant Green's function (Eq. (3.4)), we first need to calculate the Hartree Green's function G_H as well as the screened Coulomb interaction W in some approximation (traditionally RPA).

3.2.1 Hartree Green's function for the two-site Hubbard model

The Hartree Green's function is calculated from the non-interacting Hamiltonian and the Hartree potential, which means in the two-site Hubbard model Hamiltonian (1.14), we put $u = 0$ and then add V_H, the spin-independent Hartree potential at vanishing external perturbation ($\varphi = 0$):

$$
H = -t \sum_{\substack{i \neq j \\ i,j=1,2}} \sum_{\sigma} c_{i\sigma}^\dagger c_{j\sigma} + \epsilon_0 \sum_{\sigma, i=1,2} n_{i\sigma} + V_{ij}^H,
\tag{3.5}
$$

and

$$
V_H(3) = -i \int d4 \, v(3^+, 4) G(4, 4^+; [\varphi])|_{\varphi=0}
\tag{3.6}
$$

The diagonal of the Green's function matrix $G(4, 4^+; [\varphi])|_{\varphi=0}$ is simply the density ρ. This can be readily seen from the definition of the Green's function, which is $-iG(1, 1^+) = \langle \Psi_0^N | T[\psi(1) \psi^\dagger(1^+)] | \Psi_0^N \rangle = \langle n(1) \rangle$. From this, we can interpret the physical meaning of the Hartree potential: If we consider there is one electron at space and time $(x_3 t_3)$, this electron feels instantaneously the electrostatic potential at r_4 that arises from all electrons at all space points. In fact, in the two-site Hubbard model, the charge density is known. We already gave the ground state with only one spin-up electron on one site. Therefore the electron density at any site is $1/2$, so that $V_{ij}^H = (u/2)\delta_{ij}$. We can also calculate V_H from its definition, in which case we need to write all the quantities into the discrete form in our model:

$$
\begin{aligned}
V_{ij}^H(t_3) &= -i \int dt_4 \sum_{kl} v_{ijkl} \delta(t_3 - t_4) \sum_{\sigma} G_{kl\sigma}(t_4, t_4^+) \\
&= -iu\delta_{ij} \sum_{\sigma} G_{ii\sigma}(t_3, t_3^+) = \frac{u}{2} \delta_{ij}
\end{aligned}
\tag{3.7}
$$

Next, by replacing V_{ij}^H in the Hamiltonian of Eq. (3.5), we can get our new Hamiltonian for calculating the Hartree Green's function. The process is the same as the calculation of the exact Green's function in chapter 1.[1] Here we show the results of this Hartree Green's function at vanishing external perturbation:

In site basis, we obtain:

$$G^H(\omega) = \begin{pmatrix} G_{11\uparrow}^H & G_{12\uparrow}^H & 0 & 0 \\ G_{21\uparrow}^H & G_{22\uparrow}^H & 0 & 0 \\ 0 & 0 & G_{11\downarrow}^H & G_{12\downarrow}^H \\ 0 & 0 & G_{21\downarrow}^H & G_{22\downarrow}^H \end{pmatrix}, \tag{3.8}$$

where

$$G_{ij\uparrow}^H(\omega) = \frac{(-1)^{i-j}}{2}\left[\frac{1}{\omega - (\epsilon_0 + t + u/2) + i\eta} + \frac{(-1)^{i-j}}{\omega - (\epsilon_0 - t + u/2) - i\eta}\right] \tag{3.9}$$

$$G_{ij\downarrow}^H(\omega) = \frac{(-1)^{i-j}}{2}\left[\frac{1}{\omega - (\epsilon_0 + t + u/2) + i\eta} + \frac{(-1)^{i-j}}{\omega - (\epsilon_0 - t + u/2) + i\eta}\right]. \tag{3.10}$$

In bonding-antibonding basis, we get:

$$G^H(\omega) = \begin{pmatrix} G_{bb\uparrow}^H & 0 & 0 & 0 \\ 0 & G_{bb\downarrow}^H & 0 & 0 \\ 0 & 0 & G_{aa\uparrow}^H & 0 \\ 0 & 0 & 0 & G_{aa\downarrow}^H \end{pmatrix}, \tag{3.11}$$

where

$$G_{bb\uparrow}^H(\omega) = \frac{1}{\omega - (\epsilon_0 - t + u/2) - i\eta} \tag{3.12}$$

$$G_{bb\downarrow}^H(\omega) = \frac{1}{\omega - (\epsilon_0 - t + u/2) + i\eta} \tag{3.13}$$

$$G_{aa\uparrow}^H(\omega) = \frac{1}{\omega - (\epsilon_0 + t + u/2) + i\eta} \tag{3.14}$$

$$G_{aa\downarrow}^H(\omega) = \frac{1}{\omega - (\epsilon_0 + t + u/2) + i\eta}. \tag{3.15}$$

The spectral function calculated from the Hartree Green's function is shown in Fig. (3.2).

3.2.2 Random-phase approximation of the screened Coulomb interaction

The physical meaning of the screened Coulomb interaction is related the polarizability, i.e., the possibility for our system to be polarized. In real space, the expression for the

---

[1]Write the Hamiltonian in the site basis, and then calculate all the wavefunctions and energies. After that, we construct the Hartree Green's function in the site basis.
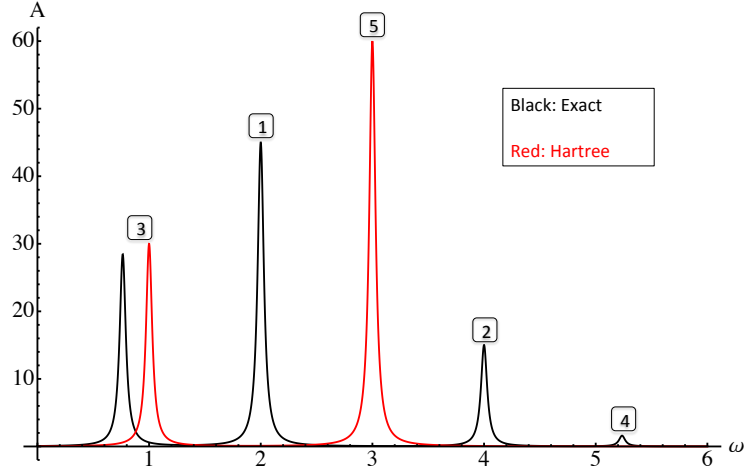
Figure 3.2: The comparison between the spectral function for electron addition calculated from the Hartree Green's function and the exact Green's function. Here $u = 2$, $\epsilon_0 = t = 1$. In the Hartree spectrum, we only get two peaks appearing at $\omega = 1$ (red peak 3) and $\omega = 3$ (peak 5). Because in the non-interacting Green's function, we got two peaks at $\omega = 0$ and $\omega = 2$ (see Fig. (2.4)), and for the Hartree Green's function, all the peaks shift by $V_H = u/2$.

RPA polarizability is

$$P(xx', t) = -iG(xx', t)G(x'x, -t). \tag{3.16}$$

This describes the creation of electron-hole pairs. i.e., if t is positive, $-t$ will be negative and vice versa, so that we have always one electron and one hole Green's function (see Eq. (1.2)).

In the two-site Hubbard model, we only have one spin-up electron in our system. The only possibility for our system to be polarized is this spin-up electron. Even when we put the external potential, there are no other electrons which can modify the Coulomb interaction in our system. So to calculate the polarizability for our model, the only thing we need is the non-interacting spin-up block of the Green's function (Eq. (2.8)). Therefore, we can predict that the result of the polarizability matrix will only contain the spin-up block.

In chapter 2, we already calculated the Green's function $G_{ij\sigma}(\omega)$ in the site basis and in the frequency domain (Eq. (2.5)). So we need to transform the polarizability into

25

frequency domain:

$$
\begin{aligned}
P_{ij\sigma}(\omega) &= F[P_{ij\sigma}(t)] = -iF[G_{ij\sigma}(t)G_{ji\sigma}(-t)] \\
&= \frac{-i}{2\pi}G_{ij\sigma}(\omega) * G_{ji\sigma}(-\omega) = \frac{-i}{2\pi}\int_{-\infty}^{+\infty} dz\, G_{ij\sigma}(z)G_{ji\sigma}(\omega+z) \quad (3.17)
\end{aligned}
$$

where $*$ means the convolution of two functions and z can be any complex number.

From this equation, we can get the polarizability matrix reading as:

$$
P^{RPA}(\omega) = \begin{pmatrix} P_{11\uparrow} & P_{12\uparrow} & 0 & 0 \\ P_{21\uparrow} & P_{22\uparrow} & 0 & 0 \\ 0 & 0 & 0 & 0 \\ 0 & 0 & 0 & 0 \end{pmatrix}, \quad (3.18)
$$

where

$$
P_{ij\uparrow}(\omega) = \frac{(-1)^{(i-j)}}{4}\left(\frac{1}{\omega - 2t + i\eta} - \frac{1}{\omega + 2t - i\eta} \right). \quad (3.19)
$$

The definition of the RPA screened Coulomb interaction is

$$
W_{RPA} = v + vPW_{RPA}. \quad (3.20)
$$

We can understand this equation from the physical meaning of W_{RPA}. Originally, $W = v + vPv + vPvPv + ...$ which means the bare Coulomb interaction v is first screened by another electron-hole pair and the screened interaction becomes $W = v + vPv$. Then our system can be screened again by another electron-hole pair, which induces $W = v + vPv + vPvPv$. We can excite as many electron-hole pairs as we have electrons in our system. Therefore we can say the screening propagates with the number of electrons,[1] which allows us to write Eq. (3.20).

In our two-site Hubbard model, we can write this equation in the site basis as:

$$
W_{ij}^{RPA}(\omega) = [1 - uP_{ij}^{RPA}(\omega)]^{-1}u, \quad (3.21)
$$

where

$$
P_{ij}^{RPA}(\omega) = \sum_{\sigma} P_{ij\sigma}^{RPA}(\omega). \quad (3.22)
$$

Then we have the result for $W_{RPA}(\omega)$ matrix

$$
W_{RPA}(\omega) = \frac{u}{1 - 2uP}\begin{pmatrix} 1 - uP & uP \\ uP & 1 - uP \end{pmatrix}, \quad (3.23)
$$

where $P = P_{11\uparrow}(\omega) = \frac{1}{4}\left(\frac{1}{\omega - 2t + i\eta} - \frac{1}{\omega + 2t - i\eta} \right)$.

---

[1] Actually in this two-site Hubbard model, we can calculate the exact screened Coulomb interaction W_{exact} due to the one electron in our system. When there is only one electron, $W_{exact} = v + vPv$. We will introduce and discuss this quantity later in chapter 4.

Therefore, we have all the W_{RPA} matrix elements in the site basis:

$$W_{12}^{RPA}(\omega) \;=\; \frac{-u^2 t}{\omega^2 - 2ut - (2t - i\eta)^2} = W_{21}(\omega) \tag{3.24}$$

$$W_{11}^{RPA}(\omega) \;=\; u + \frac{u^2 t}{\omega^2 - 2ut - (2t - i\eta)^2} = W_{22}(\omega). \tag{3.25}$$

Then we transform W_{RPA} into the bonding-antibonding basis via the basis transformation equation (Eq. (2.10)), we obtain:

$$W_{bb}^{RPA}(\omega) \;=\; \frac{u}{2} \tag{3.26}$$

$$W_{aa}^{RPA}(\omega) \;=\; \frac{u}{2} + \frac{u^2 t}{\omega^2 - 2ut - (2t - i\eta)^2} \tag{3.27}$$

$$W_{ba}^{RPA}(\omega) \;=\; W_{ab}^{RPA}(\omega) = 0. \tag{3.28}$$

3.2.3 Cumulant expansion in site basis and bonding-antibonding basis

As we mentioned before, the cumulant expansion involves a decoupling of the matrix elements of the Green's function. Model calculations designed for strongly correlated systems, namely dynamical mean field theory (DMFT) [16] that involve similar ideas, are always done in site basis. But in silicon, Bloch functions were chosen. How important is this? This has never been studied before. We will discuss the basis effects in this chapter.

Now, we have everything to calculate the cumulant Green's function in Eq. (3.4) for the two-site Hubbard model. First, we work in the bonding-antibonding basis because both $G_H(\omega)$ and $W_{RPA}(\omega)$ are exactly diagonal in this basis.

We need to write $W_{RPA}(\omega)$ in the time domain via Fourier transform:

$$W_{bb}^{RPA}(\tau) \;=\; \frac{u}{2}\delta(\tau) \tag{3.29}$$

$$W_{aa}^{RPA}(\tau) \;=\; \frac{u}{2}\delta(\tau) - i\frac{u^2 t}{2h}(\theta(\tau)e^{-ih\tau} + \theta(-\tau)e^{ih\tau}), \tag{3.30}$$

where we define $h^2 = 4t^2 + 2ut$. Here and hereafter, τ is always defined as $t_1 - t_2$.

Here we choose the calculation of $G_{aa\uparrow}(\omega)$ as one example to demonstrate how to get the whole Green's function matrix, and therefore also the spectral function. $G_{aa\uparrow}(\omega)$ describes the situation when we add one spin-up electron to our system, i.e., it is the electron propagation. So we know the time ordering should be $t_1 > t_2$ and we should use W_{aa} and $G_{aa\uparrow}^H$.

First we need to calculate the integral in Eq. (3.4)

$$\int_{t_2}^{t_1} dt_3 \int_{t_2}^{t_3} dt_4 W_{aa}(t_3^+ t_4) = -iA + iAe^{-ih(t_1 - t_2)} - Ah(t_1 - t_2), \tag{3.31}$$

where we define $A = \frac{u^2 t}{2h^3}$.

$$G_{aa\uparrow}^{C}(\tau)|_{\varphi=0} = G_{aa\uparrow}^{H}(\tau)e^{-A}e^{iAh\tau}e^{Ae^{-ih\tau}}. \tag{3.32}$$

Expanding the last term into a Taylor series[1]

$$e^{Ae^{-ih\tau}} = 1 + Ae^{-ih\tau} + \frac{A^2}{2}e^{-i2h\tau} + \frac{A^3}{6}e^{-i3h\tau} + ..., \tag{3.33}$$

we can Fourier transform $G_{aa\uparrow}^{C}(\tau)|_{\varphi=0}$ into the frequency domain:[2]

$$
\begin{aligned}
G_{aa\uparrow}^{C}(\omega)|_{\varphi=0} = {} & \frac{e^{-A}}{\omega - (\epsilon_0 + t + u/2 - Ah) + i\eta} + \frac{Ae^{-A}}{\omega - (\epsilon_0 + t + u/2 - Ah + h) + i\eta} \\
& + \frac{A^2 e^{-A}/2}{\omega - (\epsilon_0 + t + u/2 - Ah + 2h) + i\eta} + \frac{A^3 e^{-A}/6}{\omega - (\epsilon_0 + t + u/2 - Ah + 3h) + i\eta} \\
& + ...
\end{aligned}
\tag{3.34}
$$

Similarly we can get all other elements in the bonding-antibonding basis (paying attention to the time-ordering). Here and hereafter, we only write out the cumulant expansion to the first order:[3]

$$
\begin{aligned}
G_{bb\uparrow}^{C}(\omega)|_{\varphi=0} &= \frac{1}{\omega - (\epsilon_0 - t) - i\eta} \tag{3.35} \\[2mm]
G_{bb\downarrow}^{C}(\omega)|_{\varphi=0} &= \frac{1}{\omega - (\epsilon_0 - t + u/2) + i\eta} \tag{3.36} \\[2mm]
G_{aa\uparrow}^{C}(\omega)|_{\varphi=0} &= \frac{e^{-A}}{\omega - (\epsilon_0 + t + u/2 - Ah) + i\eta} \\
&\quad + \frac{Ae^{-A}}{\omega - (\epsilon_0 + t + u/2 - Ah + h) + i\eta} \tag{3.37} \\[2mm]
G_{aa\downarrow}^{C}(\omega)|_{\varphi=0} &= \frac{e^{-A}}{\omega - (\epsilon_0 + t + u/2 - Ah) + i\eta} \\
&\quad + \frac{Ae^{-A}}{\omega - (\epsilon_0 + t + u/2 - Ah + h) + i\eta}. \tag{3.38}
\end{aligned}
$$

When we derived Eq. (3.3), we knew that we would only need the diagonal elements of the screened interaction, but W is not necessarily diagonal. In the site basis, we used only the diagonal elements W_{11} and W_{22} to calculate $G_{ii\sigma}^{C}$. The problem is that the Hartree Green's function matrix in the site basis is not diagonal (Eq. 3.8), in which case

---

[1]That is where the name cumulant expansion comes from.

[2]Here we use the Fourier transform equations and the differential form of the step function as defined in chapter 1

[3]Actually we can follow a rule to write out the higher order terms. In addition, we should pay attention on the + sign on the time index in W during the integral.

we will only take into account the diagonal elements of G_H to calculate the diagonal elements of G^C:[1]

$$
\begin{aligned}
G_{ii\uparrow}^C(\omega) &= \frac{e^{-A}/2}{\omega - (\epsilon_0 + t + u/2 - Ah) + i\eta} + \frac{e^{-A}/2}{\omega - (\epsilon_0 + t + u/2 - Ah + h) + i\eta} \\
&+ \frac{e^{-A}/2}{\omega - (\epsilon_0 - t - u/2 + Ah) - i\eta} + \frac{e^{-A}/2}{\omega - (\epsilon_0 - t - u/2 + Ah - h) - i\eta} \\
G_{ii\downarrow}^C(\omega) &= \frac{e^{-A}/2}{\omega - (\epsilon_0 + t + u/2 - Ah) + i\eta} + \frac{e^{-A}/2}{\omega - (\epsilon_0 + t + u/2 - Ah - h) + i\eta} \\
&+ \frac{e^{-A}/2}{\omega - (\epsilon_0 - t + u/2 - Ah) + i\eta} + \frac{e^{-A}/2}{\omega - (\epsilon_0 - t + u/2 - Ah + h) + i\eta}.
\end{aligned}
$$

Comparing the results in different basis sets, we find that for the hole Green's function, the cumulant expansion in the bonding-antibonding basis is the same as the exact result (see Eq. (2.11) and (3.35)). In the site basis, on the other hand, there are a shift and also satellites because of the so-called self-screening problem [13].[2] Because there is only one quasiparticle peak and no satellites for the exact hole Green's function, we will mainly deal with the electron Green's function.

The performance of the cumulant Green's function in different basis sets is shown in Fig. (3.3).

From the comparison between different basis sets, we can get the conclusion: For the hole Green's function, the bonding-antibonding basis will give us the exact result, but in the site basis, we encounter the self-screening problem. Therefore the bonding-antibonding basis is better than the site basis for the hole Green's function. For the electron Green's function, the different basis sets give different results, but it is not clear which basis is better. We only get two quasiparticle peaks (instead of three in Fig. (2.2)) in the cumulant expansion because we start from the two-peak Hartree Green's function. This is consistent with the literature [7], the cumulant expansion does not work well for quasiparticle peaks.

---

[1]Actually the diagonal elements of G_H in the site basis already contain all the information needed for the calculation of the spectral function, because

$$
G_{11\uparrow}^H + G_{22\uparrow}^H + G_{11\downarrow}^H + G_{22\downarrow}^H = G_{bb\uparrow}^H + G_{bb\downarrow}^H + G_{aa\uparrow}^H + G_{aa\downarrow}^H.
$$

[2]When we remove the only electron from our system, there is nothing left to be screened, so there should not be any satellite. If there is still a satellite left, that means the hole is screened by itself.
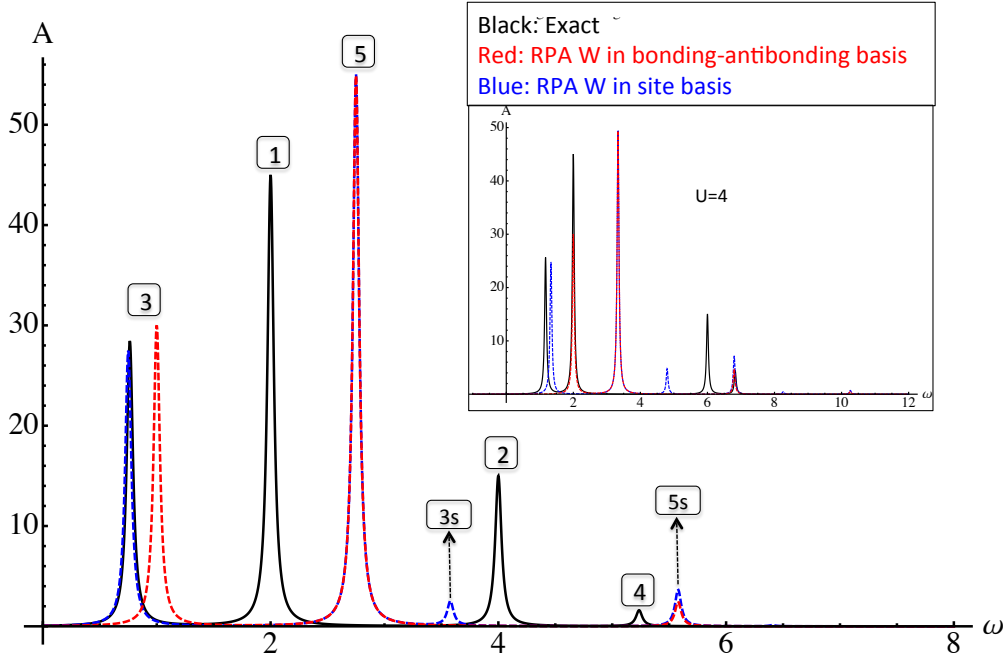
Figure 3.3: Spectral function for electron propagation in the site basis and the bonding-antibonding basis when $\epsilon_0 = t = 1$ and $u = 2$ ($u = 4$ in the inset plot). For peak 1 and 2 in the exact spectrum, both basis sets give us the same result (peak 5). This peak creates the cumulant satellite series 5s (the intensity of other satellites is too small to be seen). For peak 3 in the exact spectrum, the site basis gives us the cumulant satellites (peak 3s) with a small shift for the quasiparticle peak. But peak 3 in the bonding-antibonding basis just gets a shift without creating any cumulant satellite. Therefore form this comparison, we cannot say which basis is better. We expect the blue peak 3 give some intensity to the satellite at the same position as the original satellite peak (peak 4). But the satellite 3s will always be at the smaller energy scale. The red peak 3 does give any satellite, which means all the red satellites come from the red peak 5 instead of red 3. When $u = 4$, both red and blue curves become worse.

Chapter 4

Performance of the cumulant expansion and the combination with GW quasiparticle correction

In this chapter, we present the spectral functions by comparing the approximate results with the exact one. For each comparison, we give a brief discussion as well as the conclusion. In the first section, we compare the cumulant spectrum calculated from the RPA W with the spectrum calculated from the exact W. In the second section, we induce the GW quasiparticle correction.

4.1 Cumulant expansion with the exact screened Coulomb interaction

As we mentioned before, in a real system (e.g. bulk silicon) we cannot calculate the exact ground state. You may ask in that case, how can we calculate the Hartree Green's function?[1] Actually in the real system, the researchers use the density functional theory (DFT), which has a very good performance in calculating the density of electrons and therefore the Hartree Green's function. In the real system, it is also impossible to calculate the exact screened Coulomb interaction W_{exact}. This is the reason why we use W_{RPA} as people did in real materials. But for the two-site Hubbard model with only one electron in our system, it is possible to calculate W_{exact} from Eq. (4.1), because there is no induced potential when we excite the only one electron in our system, hence

$$W_{exact} = v + vPv. \tag{4.1}$$

Compared with the RPA case, we just replace W_{RPA} in the right hand of Eq. (3.20)

---

[1]If we do not know the ground state, we cannot calculate the density and hence the Hartree Green's function as we did in chapter 2.

with the bare Coulomb interaction v. The result is:

$$W_{exact}(\omega) = \begin{pmatrix} u + u^2 P & -P \\ -P & u + u^2 P \end{pmatrix}, \tag{4.2}$$

where $P = P_{11\uparrow}(\omega) = \frac{1}{4}\left(\frac{1}{\omega - 2t + i\eta} - \frac{1}{\omega + 2t - i\eta}\right)$.

In the bonding-antibonding basis we obtain:

$$W_{bb}^{exact}(\omega) = \frac{u}{2} \tag{4.3}$$

$$W_{aa}^{exact}(\omega) = \frac{u}{2} + \frac{u^2}{4}\left(\frac{1}{\omega - 2t + i\eta} - \frac{1}{\omega + 2t - i\eta}\right) \tag{4.4}$$

$$W_{ba}^{exact}(\omega) = W_{ab}^{exact}(\omega) = 0. \tag{4.5}$$

With this exact screened Coulomb interaction, we can calculate the new cumulant Green's function with W_{exact} instead of W_{RPA}, which can be used to investigate the performance of the random-phase approximation as shown in Fig. (4.1). Actually the only thing which is different from the case of RPA (in both basis sites) is the pole of W and the corresponding oscillation strength: In the RPA case, the pole of W is at h (see Eq. (3.23)), but in W_{exact} the pole is at $2t$ (see Eq. (4.2)). What we need to do here is just to replace all the h quantities in the RPA W by $2t$, then W_{RPA} becomes W_{exact}. The pole of W determines the plasmon energy in our system (the energy difference between two cumulant satellites) and the oscillation strength determines the probability for this plasmon excitation to happen. Here, we show the cumulant expansion spectrum with W_{exact} in Fig. (4.1).

4.2 GW corrections for the quasiparticle peaks

First, we give the spectral function calculated from GW with W_{RPA} and W_{exact} (Fig. (4.2)). From this figure, we can see the splitting of peak 5 into three peaks. Moreover, one peak goes to peak 2 another two peaks go to around peak 1.

4.2.1 GW corrections with RPA screened Coulomb interaction

In this part, we use the RPA screened Coulomb interaction W_{RPA} for the calculation of both the cumulant expansion and GW correction. Then we combine the cumulant expansion and the GW correction to get the spectrum shown in Fig. (4.3). In the solids (e.g. silicon), we have the assumption that the quasiparticle shift in the cumulant expansion (Ah term in Eq. (3.32)) is equal to the energy difference between GW quasiparticle energy and Hartree quasiparticle energy (i.e., $Ah = \epsilon_{GW} - \epsilon_{Hartree}$). Here, we use the same assumption to correct our quasiparticle peaks in the cumulant expansion.

4.2.2 GW corrections with the exact screened Coulomb interaction

In this section we use W_{exact} everywhere instead of W_{RPA} to plot Fig. (4.4).
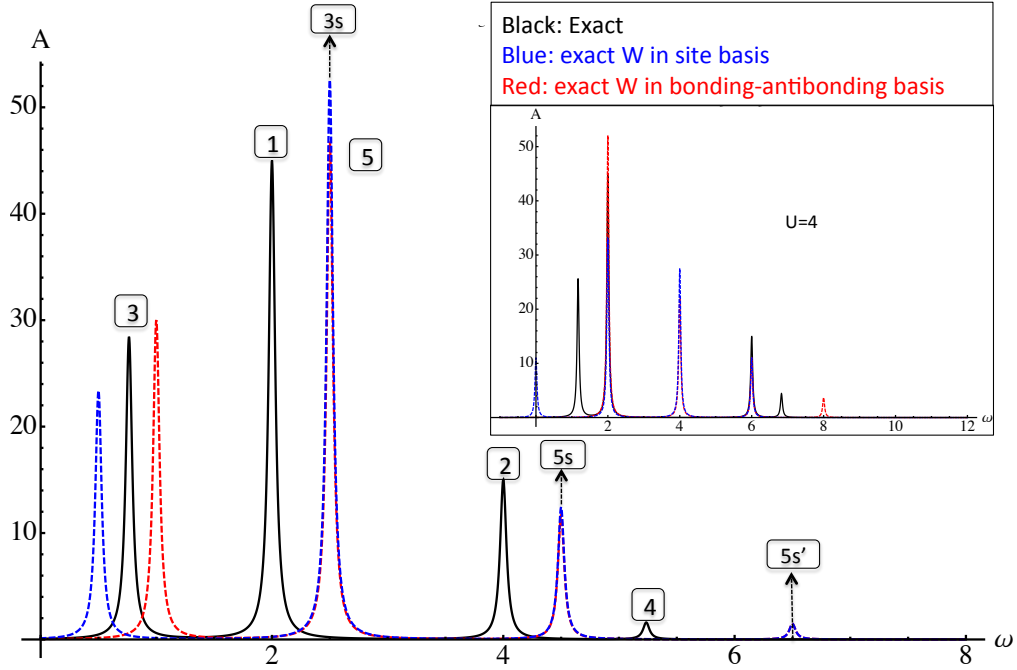
Figure 4.1: The spectral function calculated for electron addition from the cumulant Green's function with the exact screened interaction under the condition that $\epsilon_0 = t = 1$ and $u = 2$ ($u = 4$ for the inset plot). First: Compared with Fig. (3.3) in the site basis (blue curve), peak 3 has a bigger shift, also it gives more intensity to the satellite 3s. The same thing happens to peak 5 which gives a lot of intensity to the satellite 5s. Even the second-order satellite 5s' gets enough intensity to be identified. Second: In the bonding-antibonding basis (red curve), peak 3 does not create any cumulant satellite and peak 5 gives a lot of intensity to its first-order satellite 5s and second-order satellite 5s'. Third: When the Coulomb interaction becomes stronger (the inset plot), the performance become worse. In site basis (blue curve in the inset), peak 3 shifts to $\omega = 0$ and its satellite (3s) is at $\omega = 2$ (degenerate with peak 5). The other quasiparticle peak in site basis (red peak at $\omega = 2$) gives a remarkable strength to its first order satellite at $\omega = 4$, as well as the second order satellite at $\omega = 6$, and even the third-order satellite at $\omega = 8$. Here we can see the energy difference between different order satellites is $2t$ when we use W_{exact}. In the bonding-antibonding basis (red curve in the inset plot), we can only recognize one quasiparticle peak which is at $\omega = 2$ and its two satellites at $\omega = 4$ and $\omega = 6$, respectively. Fourth: We do see some differences between the performance of different basis sets but it is not enough to tell which basis is better.

33
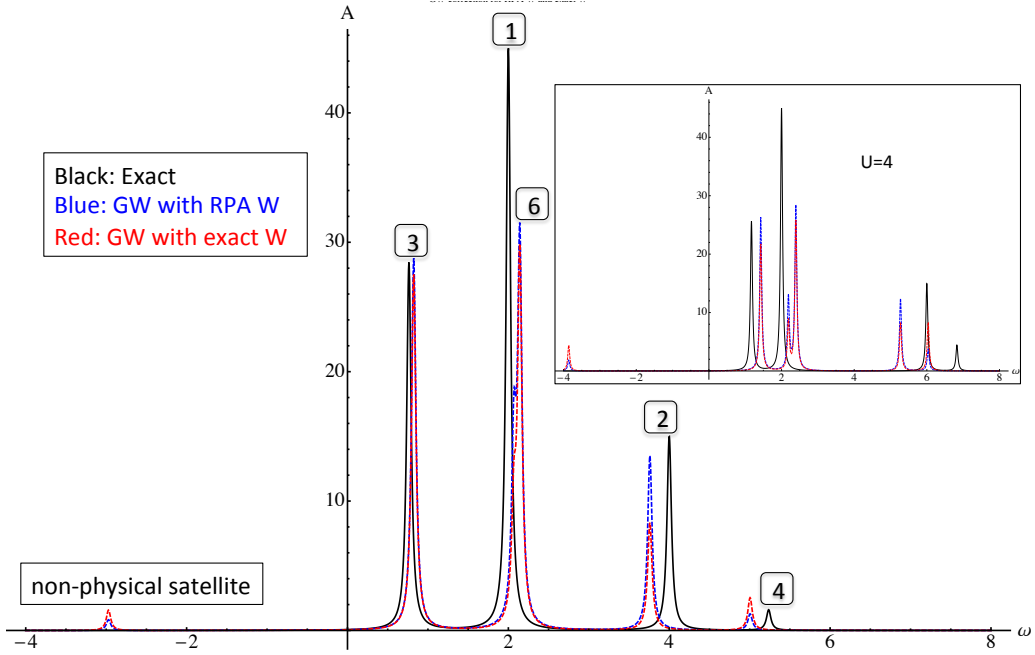
Figure 4.2: Comparison between the exact spectrum and the GW result (W_{exact} and W_{RPA}). First: Compared to the cumulant expansion (Fig. (3.3)), the quasiparticle peaks become better. However, it gives a very bad description of the satellite (non-physical satellite appears), which is consistent with the literature on the GW approximation [8]. Second: For the quasiparticle peaks when $u = 2$, peak 3 is very similar to the exact peak. Peak 1 in the exact spectrum here becomes peak 6 in GW spectrum. Actually peak 6 is splitted into two peaks. For peak 2, W_{RPA} performs better than W_{exact}. Third: We can see there is a non-physical satellite for both W_{RPA} and W_{exact}. We say it to be non-physical because in the case of adding one electron to our system, the satellite should appear at a higher energy level than the quasiparticle energy. Fourth: In the case of strong interaction (inset figure), the performance becomes worse because there are more satellites identifiable and peak 6 splits into two separate peaks.

34
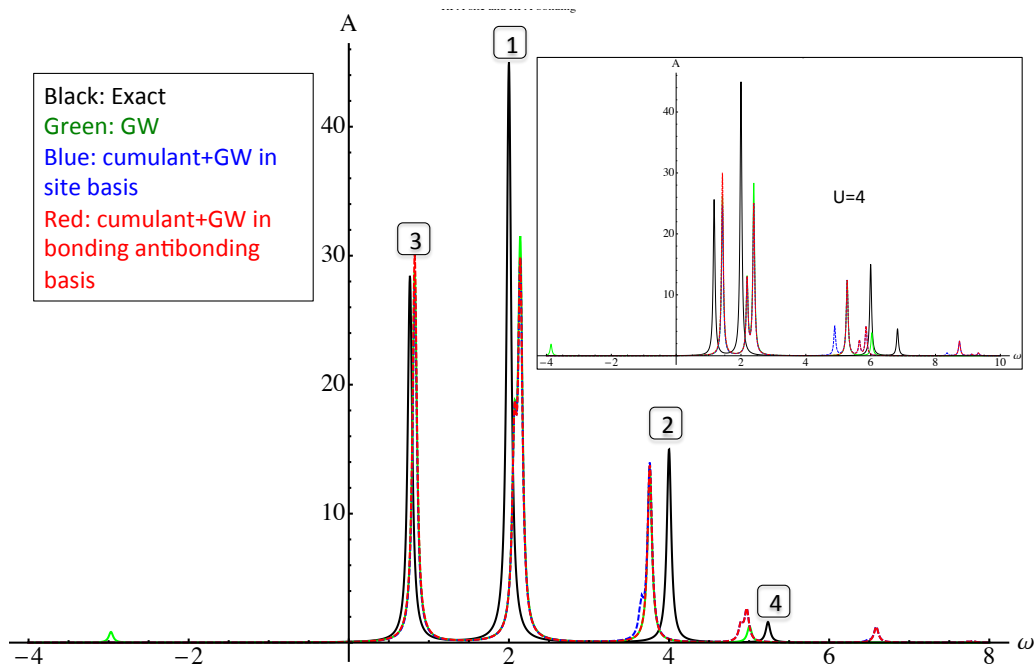
Figure 4.3: The spectral function for electron addition calculated from the cumulant+GW approach with the RPA screened Coulomb interaction. Here we set $\epsilon_0 = t = 1$ and $u = 2$ ($u = 4$ for the inset plot). We can see the improvement compared with the pure cumulant (Fig. (3.3)) and the pure GW (green curve in Fig. (4.3)). Both quasiparticle peaks and satellites are quite similar to the exact spectrum. In the strong interaction system (the inset plot), the performance becomes worse, especially in site basis that shows one more satellite than in bonding-antibonding basis. Here, the bonding-antibonding basis performs a little bit better than the site basis.
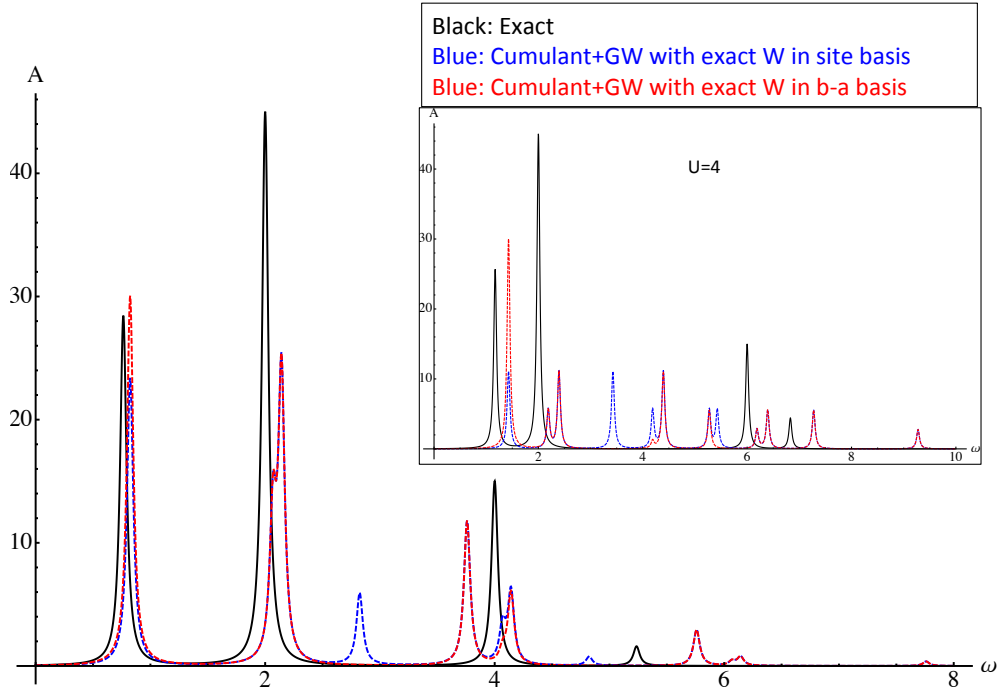
Figure 4.4: Cumulant+GW approach with W_{exact} in site basis and bonding-antibonding basis. First: In bonding-antibonding basis, W_{exact} (red curve in Fig. (4.4)) performs as well as W_{RPA} (red curve in Fig. (4.3)), and we cannot tell which one is better. But in site basis, RPA W performs better (comparison between blue curve in Fig. (4.4)) and (4.3)). At the beginning, we expected a better performance of W_{exact} compared to W_{RPA}, but here W_{exact} performs not very well, or at least, not better than RPA W. We think that this happens because in the cumulant expansion approximation, we put approximations on all the quantities involved (including G_H and W) consistently. If we only introduce one exact quantity in this system, the results can become worse because the approximation is less consistent. We can also say that RPA performs well enough, which is why the researchers work with RPA traditionally. Second: From the inset figure, we can clearly see how bad the performance for W_{exact} in both basis when the interaction is strong ($u = 4$). GW calculations with different W did not give such a bad result (see Fig. (4.2)), so the bad performance here should come from the cumulant expansion. When we calculate the cumulant expansion with the W_{exact} the quasiparticle will always give more intensity to the satellites compared to W_{RPA} case, due to different poles in W. Here, the only peak which is similar to the exact quasiparticle peak is peak 3 in bonding-antibonding basis, because this peak does not give any intensity to the satellite (see Eq. (3.36)). Third: From the comparison between different basis sets, we find that the bonding-antibonding basis performs better than the site basis, because the site basis always gives more satellites than the bonding-antibonding basis.

Chapter 5

Conclusion

The main idea of this work is to investigate the performance of the combination of the cumulant expansion and GW quasiparticle corrections in a finite system (the two-site Hubbard model). That is to say, we use the good performance of GW for the description of quasiparticle peaks and drop its bad performance for satellites. Instead, we use the cumulant expansion to describe the satellite structure. Unfortunately, the performance of this approach for the two-site Hubbard model is not as good as for bulk silicon, since in such a finite system (one electron in the ground sate), the plasmon excitation cannot propagate as in the case of an infinite system.

The cumulant expansion approximation is basis-set dependent, and from our study, the basis does affect the spectrum, especially for hole propagation. In bonding-antibonding basis, the cumulant spectrum for the hole Green's function is always the same as the exact spectrum, but in site basis, there is a self-screening problem similar to what GW suffers. For the electron Green's function, when working with the pure cumulant expansion, we cannot tell which basis is better. But when we work with the combined approximation of cumulant satellites and GW quasiparticles, the bonding-antibonding basis performs better than the site basis.

From the comparison between the cumulant expansion calculated with the exact screened Coulomb interaction and the RPA W, the conclusion is that RPA W performs very well, even better than the exact W in some cases when compared to the exact spectrum. We think that this is a matter of consistency. If we use only one of the quantities involved in this approach in its exact version, the final performance can be worse.

The combination of the cumulant expansion with GW quasiparticles performs better than the individual approach. We can clearly see the improvement of both quasiparticle peaks and satellites in the spectrum. But because GW itself does not perform very well for the two-site Hubbard model for the quasiparticle peaks at strong interaction [13], we cannot expect any better performance in our work for the quasiparticle peaks. For the satellite structure, we expected a better performance relative to the work of Romaniello *et al.*. Although we avoid the problem of non-physical satellites, the position of some satellite peaks could still be improved.

Now, I am thinking about how to improve our approach based on the performance we already discussed:

First, we can study the approximations involved in the cumulant expansion. As I have explained, the main approximations involved are the so-called linearization (Eq. (3.2)) and diagonalization (Eq. (3.3)) approximations. We have the exact solution of Eq. (3.3), which already includes both approximations. The result is not good enough for the two-site Hubbard model. How good would it be if we were able to avoid some approximations? A promising step for future investigation could be to use the solution including linearization and diagonalization to iterate the equation with only linearization (Eq. (3.2)). Namely, we use the solution of (3.3) and put it in the right hand side of (3.2) to recalculate the Green's function. If this iteration would converge, it would be better than the cumulant Green's function G^C (Eq. (3.4)). If we successfully found a better solution, we could even iterate the equation of motion of the one-particle Green's function (Eq. (3.1)) without using any other approximations. However, as P. A. M. Dirac stated in 1929: the difficulty is that the application of the laws (in physics) always leads to equations much too complicated to be soluble. Another possible method is to change the model a little bit, which may allow us to understand the performance of our approach better. In the two-site Hubbard model we used in this work, there is only one satellite peak for the electron propagation (as measured in inverse photoemission). For the hole propagation, there is only one quasiparticle peak without any satellite. The system is too small to investigate the satellite performance in our approach. We could instead, use the two-site Hubbard model with two electrons in the future or two sites with more orbitals. In these cases, we would be able to see the propagation of the plasmon excitations and therefore more satellites. We expect better performance for our approach in a larger system. However, in this work we intentionally studied a system where the approach is supposed to perform badly to analyze its failures and get insights for constructing even better method in the future.

In this thesis, I have studied a lot of theories in many-body physics. From the very beginning of the second quantization to the many-body Green's function and a series of approximate theories (Hartree-Fock approximation, GW approximation, and the cumulant expansion), as well as the Hubbard model for solving the many-body problem. I have considered a possible explanation for the one-particle Green's function matrix elements in the two-site Hubbard model via energy-level diagrams. By studying the performance of combining the cumulant expansion with GW quasiparticle corrections in the two-site Hubbard model, I learned a lot of mathematical strategies to solve different types of equations and how to analyze the mathematical results from the physics point of view. A particularly important investigation we have done in this work is the analysis the basis-set effects in the cumulant expansion approximation, which has not yet been done by others before.

This is what I have started to learn in this thesis and I would like to continue my work in this field (theoretical spectroscopy) during my PhD period.

References

[1] Julien Vidal, Silvana Botti, Pär Olsson, Jean-Fran çois Guillemoles, and Lucia Reining. Strong Interplay between Structure and Electronic Properties in $CuIn(\mathbf{S}, Se)_2$: A First-Principles Study. *Phys. Rev. Lett.*, 104:056401, Feb 2010. 2

[2] Wojciech Wełnic, Silvana Botti, Lucia Reining, and Matthias Wuttig. Origin of the Optical Contrast in Phase-Change Materials. *Phys. Rev. Lett.*, 98:236403, Jun 2007. 2

[3] Klochikhin A.A. Seisyan R.P. Emtsev V.V. Ivanov S.V. Bechstedt F. Furthmller J. Harima H. Mudryi A.V. Aderhold J. Semchinova O. Davydov, V.Yu. and Graul. Absorption and Emission of Hexagonal InN. Evidence of Narrow Fundamental Band Gap. *Phys. Status Solidi B*, 229:r1–r3, Feb. 2002. 3

[4] E. K. U. Gross, E. Runge, and O. Heinonen. *Many-particle theory*. A. Hilger, Bristol ; Philadelphia :, 1991. 5

[5] David C. Langreth. Singularities in the X-Ray Spectra of Metals. *Phys. Rev. B*, 1:471–477, Jan 1970. 7

[6] L. Hedin, B.I. Lundqvist, and S. Lundqvist. New structure in the single-particle spectrum of an electron gas. *Solid State Communications*, 5(4):237 – 239, 1967. 7

[7] L. Hedin. On correlation effects in electron spectroscopies and GW approximation. *J. Phys.: Condens. Matter*, 11(42):R489, 1999. 8, 29

[8] Mark S. Hybertsen and Steven G. Louie. Electron correlation in semiconductors and insulators: Band gaps and quasiparticle energies. *Phys. Rev. B*, 34:5390–5413, Oct 1986. 8, 34

[9] Matteo Guzzo, Giovanna Lani, Francesco Sottile, Pina Romaniello, Matteo Gatti, Joshua J. Kas, John J. Rehr, Mathieu G. Silly, Fausto Sirotti, and Lucia Reining. Valence Electron Photoemission Spectrum of Semiconductors: Ab Initio Description of Multiple Satellites. *Phys. Rev. Lett.*, 107:166401, Oct 2011. 8, 22, 23

[10] J. Hubbard. Electron Correlations in Narrow Energy Bands. *Proc. R. Soc. London, Ser. A*, 276:238–257, Nov. 1963. 8

[11] J. Hubbard. Electron Correlations in Narrow Energy Bands. II. The Degenerate Band Case. *Proc. R. Soc. London, Ser. A*, 277:237–259, Jan 1964. 8

[12] J. M. Tomczak. *Spectral and Optical Properties of Correlated Materials*. PhD thesis, Ecole Polytechnique, 2007. 11

[13] P. Romaniello, S. Guyot, and L. Reining. The self-energy beyond GW: Local and nonlocal vertex corrections. *The Journal of Chemical Physics*, 131(15):154111, 2009. 11, 29, 37

[14] Gordon Baym and Leo P. Kadanoff. Conservation Laws and Correlation Functions. *Phys. Rev.*, 124:287–299, Oct 1961. 21

[15] Giovanna Lani, Pina Romaniello, and Lucia Reining. Approximations for many-body Green's functions: insights from the fundamental equations. *New Journal of Physics*, 14(1):013056, 2012. 22

[16] Antoine Georges, Gabriel Kotliar, Werner Krauth, and Marcelo J. Rozenberg. Dynamical mean-field theory of strongly correlated fermion systems and the limit of infinite dimensions. *Rev. Mod. Phys.*, 68:13–125, Jan 1996. 27